

**BUKTI  
SUBMIT  
MANUSKRIP**



Andi Dian Permana &lt;andi.dian.permana@farmasi.unhas.ac.id&gt;

**ACS Applied Materials & Interfaces - Manuscript ID am-2022-16857x**

1 message

ACS Applied Materials &amp; Interfaces &lt;onbehalf@manuscriptcentral.com&gt;

Mon, Sep 19, 2022 at 4:13 PM

Reply-To: support@services.acs.org

To: andi.dian.permana@farmasi.unhas.ac.id

Cc: mudjahidm20n@student.unhas.ac.id, firzannainu@unhas.ac.id, rifkanurulutami@unhas.ac.id, sama21n@student.unhas.ac.id, marzamananf21n@student.unhas.ac.id, roskatp21n@student.unhas.ac.id, rangga.masri@farmasi.unhas.ac.id, andi.dian.permana@farmasi.unhas.ac.id

19-Sep-2022

Journal: ACS Applied Materials &amp; Interfaces

Manuscript ID: am-2022-16857x

Title: "Enhancement in Site-Specific Delivery of Chloramphenicol Using Bacterially Sensitive Microparticle Loaded Into Dissolving Microneedle : Potential For Enhanced Effectiveness Treatment of Cellulitis"

Authors: Mudjahid, Mukarram ; Nainu, Firzan; Utami, Rifka; Sam, Anwar; Marzaman, Ardiyah; Roska, Tri; Asri, Rangga; Himawan, Achmad; F. Donnelly, Ryan; Permana, Andi Dian

Manuscript Status: Submitted

Dear Dr. Permana:

Your manuscript has been successfully submitted to ACS Applied Materials &amp; Interfaces.

Please reference the above manuscript ID in all future correspondence or when calling the office for questions. If there are any changes in your contact information, please log in to ACS Paragon Plus with your ACS ID at <http://acsparagonplus.acs.org/> and select "Edit Your Profile" to update that information.

You can view the status of your manuscript by checking your "Authoring Activity" tab on ACS Paragon Plus after logging in to <http://acsparagonplus.acs.org/>.

## Journal Publishing Agreement and Copyright

Upon acceptance, ACS Publications will require the corresponding author to sign and submit a Journal Publishing Agreement. This agreement gives authors a number of rights regarding the use of their manuscripts. At acceptance, the corresponding author will receive an email linking through to the Journal Publishing Agreement Wizard, which helps you select the most appropriate license for your manuscript.

For more information please see: [https://pubs.acs.org/page/copyright/journals/jpa\\_faqs.html](https://pubs.acs.org/page/copyright/journals/jpa_faqs.html)

## ACS Authoring Services

Did you know that ACS provides authoring services to help scientists prepare their manuscripts and communicate their research more effectively? Trained chemists with field-specific expertise are available to edit your manuscript for grammar, spelling, and other language errors, and our figure services can help you increase the visual impact of your research.

Visit <https://authoringservices.acs.org> to see how we can help you! Please note that the use of these services does not guarantee that your manuscript will be accepted for publication.

Thank you for submitting your manuscript to ACS Applied Materials & Interfaces.

Sincerely,

Dr. Kirk Schanze

ACS Applied Materials &amp; Interfaces

-----  
PLEASE NOTE: This email message, including any attachments, contains confidential information related to peer review and is intended solely for the personal use of the recipient(s) named above. No part of this communication or

any related attachments may be shared with or disclosed to any third party or organization without the explicit prior written consent of the journal Editor and ACS. If the reader of this message is not the intended recipient or is not responsible for delivering it to the intended recipient, you have received this communication in error. Please notify the sender immediately by e-mail, and delete the original message.

As an author or reviewer for ACS Publications, we may send you communications about related journals, topics or products and services from the American Chemical Society. Please email us at [pubs-comms-unsub@acs.org](mailto:pubs-comms-unsub@acs.org) if you do not want to receive these. Note, you will still receive updates about your manuscripts, reviews, or future invitations to review.

Thank you.

**BUKTI  
REVIEW  
DARI  
REVIEWERS**



Andi Dian Permana &lt;andi.dian.permana@farmasi.unhas.ac.id&gt;

**Revision Requested for Manuscript ID am-2022-16857x**

1 message

ACS Applied Materials &amp; Interfaces &lt;onbehalf@manuscriptcentral.com&gt;

Fri, Oct 14, 2022 at 2:27 AM

Reply-To: ivanisevic-office@ami.acs.org

To: andi.dian.permana@farmasi.unhas.ac.id

13-Oct-2022

Journal: ACS Applied Materials &amp; Interfaces

Manuscript ID: am-2022-16857x

Title: "Enhancement in Site-Specific Delivery of Chloramphenicol Using Bacterially Sensitive Microparticle Loaded Into Dissolving Microneedle : Potential For Enhanced Effectiveness Treatment of Cellulitis"

Author(s): Mudjahid, Mukarram ; Nainu, Firzan; Utami, Rifka; Sam, Anwar; Marzaman, Ardiyah; Roska, Tri; Asri, Rangga; Himawan, Achmad; F. Donnelly, Ryan; Permana, Andi Dian

Dear Dr. Permana:

Thank you for submitting your manuscript for publication in ACS Applied Materials & Interfaces. The reviewer comments for the above-referenced manuscript are enclosed for your information. The reviewers indicate that the manuscript requires major revision to address a number of specific points before it can be published.

On the basis of the reviewer comments and my own assessment of the manuscript, I am willing to consider a revised version of this paper for publication in ACS Applied Materials & Interfaces pending a second round of external review. In preparing the revision, carefully consider all of the comments made by the reviewers.

We would like to receive your revision as soon as possible, by 03-Nov-2022 at the latest.

In addition to addressing the reviewers' comments, please make sure that your manuscript addresses the following issues:

1) Funding Sources: Authors are required to report ALL funding sources and grant/award numbers relevant to this manuscript. Enter all sources of funding for ALL authors relevant to this manuscript in BOTH the Open Funder Registry tool in ACS Paragon Plus and in the manuscript to meet this requirement. See [http://pubs.acs.org/page/4authors/funder\\_options.html](http://pubs.acs.org/page/4authors/funder_options.html) for complete instructions.

2) ORCID: Authors submitting manuscript revisions are required to provide their own validated ORCID iDs before completing the submission, if an ORCID iD is not already associated with their ACS Paragon Plus user profiles. This iD may be provided during original manuscript submission or when submitting the manuscript revision. You can provide only your own ORCID iD, a unique researcher identifier. If your ORCID iD is not already validated and associated with your ACS Paragon Plus user profile, you may do so by following the ORCID-related links in the Email/Name section of your ACS Paragon Plus account. All authors are encouraged to register for and associate their own ORCID iDs with their ACS Paragon Plus profiles. The ORCID iD will be displayed in the published article for any author on a manuscript who has a validated ORCID iD associated with ACS Paragon Plus when the manuscript is accepted. Learn more at <http://www.orcid.org>.

3) \*\*\*Please note that you may receive a follow-up message within one business day describing the non-scientific changes you must also make to your manuscript before you submit the revision.

4) On resubmission, please provide 2 copies of the final manuscript file:

a) The final revised manuscript file that does not contain any highlighting or editing marks. This file should be uploaded as the primary manuscript document file.

b) A marked copy of the revised manuscript that shows changes made on revision clearly highlighted. This file should be uploaded SEPARATELY FROM THE FINAL MANUSCRIPT FILE as Supporting Information for Review.

c) Do not add any highlighting or other editing marks to the supporting information file that is intended to be published with the manuscript (this file is uploaded as "supporting information for publication").

To revise your manuscript, log into ACS Paragon Plus with your ACS ID at <http://acsparagonplus.acs.org/> and select "My Authoring Activity". There you will find your manuscript title listed under "Revisions Requested by Editorial Office." Your original files are available to you when you upload your revised manuscript. If you are replacing files, please remove the old version of the file from the manuscript before uploading the new file.

When submitting your revised manuscript through ACS Paragon Plus, you will be able to respond to the comments made by the reviewer(s) in the text box provided or by attaching a file containing your detailed responses to all of the points raised by the reviewers.

Please make sure your manuscript adheres to the formatting specifications of ACS Applied Materials & Interfaces. The instructions are available to authors using the following url: <http://pubs.acs.org/page/aamick/submission/authors.html>

You may also find it helpful to look at the online version of the journal at <http://pubs.acs.org/journal/aamick>.

Thank you for considering ACS Applied Materials & Interfaces as a forum for the publication of your work.

ACS Publications uses Crossref Similarity Check Powered by iThenticate to detect instances of similarity in submitted manuscripts. In publishing only original research, ACS is committed to deterring plagiarism, including self-plagiarism. Your manuscript may be screened for similarity to published material.

With sincere regards,

Prof. Albena Ivanisevic  
Associate Editor  
ACS Applied Materials & Interfaces  
Fax: 12023509587  
email: [ivanisevic-office@ami.acs.org](mailto:ivanisevic-office@ami.acs.org)

---

Reviewer(s)' Comments to Author:

Reviewer: 1

Recommendation: Publish after minor revisions noted.

Comments:

Here are some of the comments regarding the manuscript titled "Enhancement in Site-Specific Delivery of Chloramphenicol Using Bacterially Sensitive Microparticle Loaded Into Dissolving Microneedle : Potential For Enhanced Effectiveness Treatment of Cellulitis";

1. Authors are advised to justify microparticles over nanoparticles loading into dissolved microneedle for the treatment of cellulitis.
2. Are there any choices of natural biodegradable polymers compatible with the drug chloramphenicol in this context?
3. Can the author throw some light on the stability of drug in the dissolving microneedle over time?

Additional Questions:

Is this paper in the top 20% of manuscripts in the field?: No

If this paper is not in the top 20% of manuscripts in the field: It could be improved to be in the top 20% with appropriate revisions.

Is it appealing to a broad audience?: Yes

Does the manuscript give a complete description of the procedures that could be reproduced by others in the field?: Yes

Are the literature references appropriate and up to date?: Yes

Provides significant insight into or the development of an important application: Good

Work is original and significant: Good

Conclusions adequately supported by data: Good

Clarity of presentation: Good

Potential for impact in materials science and engineering: Good

Reviewer: 2

Recommendation: Major revisions needed as noted.

## Comments:

The comment for Authors:

This study combined the dissolving microneedles (MNs) and bacteria-sensitive microparticles (MPs) for enhanced penetration and targeted delivery of chloramphenicol (CHL) to the infection site specifically. This study includes the microparticle formulation design based on the Design-Expert® application, in vitro and in vivo test on the mutant drosophila larval infection model. They provide the improvement of the antibacterial activity of MPs and higher retention duration compared to conventional cream formulation. The design of this study is interesting and experimental designs are logical and well planned. However, I have the following concerns.

1. Why the authors choose the mutant drosophila larval infection model but not animal model?
2. The particle size and the zeta potential should be defined. The zeta potential may also affect the particles contact with bacterial.
3. The degradation time of PCL is long, how does the chloramphenicol release from the MPs?
4. How does the authors evaluate the total chloramphenicol quantity in one MN patch?
5. As shown in Fig. 5C, the XRD figure show the amorphous type of chloramphenicol loaded in the MPs, is the structure and the activity the same with original one? The author should discuss about that.
6. Actually, it is suggested that the animal model is necessary.

## Additional Questions:

Is this paper in the top 20% of manuscripts in the field?: No

If this paper is not in the top 20% of manuscripts in the field: It could be improved to be in the top 20% with appropriate revisions.

Is it appealing to a broad audience?: Yes

Does the manuscript give a complete description of the procedures that could be reproduced by others in the field?: Yes

Are the literature references appropriate and up to date?: Yes

Provides significant insight into or the development of an important application: Fair

Work is original and significant: Fair

Conclusions adequately supported by data: Fair

Clarity of presentation: Fair

Potential for impact in materials science and engineering: Good

-----  
FOR ASSISTANCE WITH YOUR MANUSCRIPT SUBMISSION PLEASE CONTACT:

ACS Publications Customer Services & Information (CSI)

Email: [support@services.acs.org](mailto:support@services.acs.org)

Phone: 202-872-4357

Toll-Free Phone: 800-227-9919 (USA/Canada only)

-----  
PLEASE NOTE: This email message, including any attachments, contains confidential information related to peer review and is intended solely for the personal use of the recipient(s) named above. No part of this communication or any related attachments may be shared with or disclosed to any third party or organization without the explicit prior written consent of the journal Editor and ACS. If the reader of this message is not the intended recipient or is not responsible for delivering it to the intended recipient, you have received this communication in error. Please notify the sender immediately by e-mail, and delete the original message.

As an author or reviewer for ACS Publications, we may send you communications about related journals, topics or products and services from the American Chemical Society. Please email us at [pubs-comms-unsub@acs.org](mailto:pubs-comms-unsub@acs.org) if you do not want to receive these. Note, you will still receive updates about your manuscripts, reviews, or future invitations to review.

Thank you.



Andi Dian Permana &lt;andi.dian.permana@farmasi.unhas.ac.id&gt;

---

**Permana, Andi Dian am-2022-16857x -- Manuscript Formatting Request - Non-scientific changes**

1 message

---

**ACS Applied Materials & Interfaces** <onbehalf@manuscriptcentral.com>

Fri, Oct 14, 2022 at 12:30 PM

Reply-To: eic@ami.acs.org

To: andi.dian.permana@farmasi.unhas.ac.id

14-Oct-2022

Manuscript ID: am-2022-16857x

Manuscript Type: Article

Title: "Enhancement in Site-Specific Delivery of Chloramphenicol Using Bacterially Sensitive Microparticle Loaded Into Dissolving Microneedle : Potential For Enhanced Effectiveness Treatment of Cellulitis"

Author(s): Mudjahid, Mukarram ; Nainu, Firzan; Utami, Rifka; Sam, Anwar; Marzaman, Ardiyah; Roska, Tri; Asri, Ranga; Himawan, Achmad; F. Donnelly, Ryan; Permana, Andi Dian

Dear Dr. Permana:

You recently received a Revision Request from Prof. Albena Ivanisevic. In addition to addressing the Editor's concerns and the requests of the reviewers, please complete the following before submitting your revision:

1. Please provide an additional keywords as 5-8 keywords are required.
2. Please make sure to submit a Table Of Contents (TOC) graphic and make sure that it is placed at the end of the manuscript file.

If you intend to use highlighting, bolding, italics, or marking of any type within the manuscript to indicate changes made in response to the reviews of your manuscript, we ask that you upload the marked-up copy as a "Supporting Information For Review Only".

We look forward to receiving your revised manuscript, so that processing of your manuscript may proceed without further delay. Thank you for considering the ACS Applied Materials & Interfaces as a forum for the publication of your work.

Sincerely,

Mallikeswari Parthasarathy  
ACS Applied Materials & Interfaces

---

FOR ASSISTANCE WITH YOUR MANUSCRIPT SUBMISSION PLEASE CONTACT:

ACS Publications Customer Services &amp; Information (CSI)

Email: [support@services.acs.org](mailto:support@services.acs.org)

Phone: 202-872-4357

Toll-Free Phone: 800-227-9919 (USA/Canada only)

---

PLEASE NOTE: This email message, including any attachments, contains confidential information related to peer review and is intended solely for the personal use of the recipient(s) named above. No part of this communication or any related attachments may be shared with or disclosed to any third party or organization without the explicit prior written consent of the journal Editor and ACS. If the reader of this message is not the intended recipient or is not responsible for delivering it to the intended recipient, you have received this communication in error. Please notify the sender immediately by e-mail, and delete the original message.

As an author or reviewer for ACS Publications, we may send you communications about related journals, topics or products and services from the American Chemical Society. Please email us at [pubs-comms-unsub@acs.org](mailto:pubs-comms-unsub@acs.org) if you do not want to receive these. Note, you will still receive updates about your manuscripts, reviews, or future invitations

4/4/23, 10:30 PM

Universitas Hasanuddin Mail - Permana, Andi Dian am-2022-16857x -- Manuscript Formatting Request - Non-scientific chang...

to review.

Thank you.

**BUKTI  
SUBMIT  
HASIL  
REVIEW**



## ABSTRACT

30  
31  
32  
33  
34  
35  
36  
37  
38  
39  
40  
41  
42  
43  
44  
45  
46  
47  
48  
49  
50  
51

One of the biggest challenges in infectious disease treatment is the existence of bacterial infections in underskin wound tissue, such as cellulitis. Compared to other treatments, it is harder for antibacterial drugs to penetrate the physical barrier on the affected skin with a non-specific target, making conventional therapy for cellulitis infection more difficult and considered. In this novel research, we pioneer a combined strategy of dissolving microneedles (MNs) and bacteria-sensitive microparticles (MPs) for enhanced penetration and targeted delivery of chloramphenicol (CHL) to the infection site specifically. The polycaprolactone polymer was used to make MPs because of its sensitivity to bacterial enzyme stimuli. The best microparticle formulation was discovered and optimized using the *Design-Expert*<sup>®</sup> application. Furthermore, this study evaluated the antibacterial activity of MPs *in vitro* and *in vivo* on the mutant drosophila larval infection model. This strategy shows that improves the antibacterial activity of MPs and higher retention duration compared to conventional cream formulation, and that the inclusion of these MPs into dissolving MNs was able to greatly improve the dermatokinetic characteristics of CHL in *ex vivo* evaluation. Importantly, the antimicrobial efficacy in an *ex vivo* infection model demonstrated that, following the use of this strategy, bacterial bioburdens **decreased** by up to 99.99% after 24 hours. The findings offered a proof of concept for the enhancement of CHL dermatokinetic profiles and antimicrobial activities after its preparation into bacterial sensitive MPs and distribution by MNs. Future research should investigate *in vivo* effectiveness in an appropriate animal model.

KEYWORDS: Bacterially Sensitive Microparticles, Cellulitis, Chloramphenicol, Dissolving Microneedle, **Polycaprolactone, Dermatokinetic**

## 52 1. Introduction

53 Chronic wounds are a major global concern and are typically caused by vascular  
54 insufficiency and infection.<sup>1</sup> Infection arises as a result of microorganism growth in the wound  
55 site, resulting in a prolonged, excessive inflammatory response, delays in collagen synthesis,  
56 and tissue degradation, leading to higher patient mortality and morbidity risks.<sup>1,2</sup> Over \$50  
57 billion is spent annually on the management of chronic wounds.<sup>3</sup> Cellulitis is type of chronic  
58 wound infection located in the dermis/subcutaneous layer of the skin; it is caused by the  
59 immune system's (cytokines and neutrophils) reaction to bacteria penetrating the epidermis.<sup>4,5</sup>  
60 The location of the infection in the cutaneous tissue with no visible wound in the epidermis of  
61 the skin, is often dismissed as ordinary inflammation. **These symptoms are also common**  
62 **among the others inflammatory skin diseases**, making diagnosis of wound-related cellulitis a  
63 substantial challenge at the same time that bacterial cultivation is developing rapidly.<sup>6</sup> It is  
64 possible to increase the degree of chronic wounds that ended difficult to heal and needed an  
65 extension in treatment management.

66 The primary method for managing infected wounds is surgical debridement, which  
67 includes the removal of necrotic and wound tissue. This is usually followed by a regimen of  
68 antimicrobial medications for long-term therapy, either topically or systemically.<sup>7,8</sup>  
69 Additionally, numerous reports of several bacterial strains colonizing human skin tissue have  
70 been reported.<sup>9</sup> This is related to the interaction of different strains of bacteria, which can  
71 synergistically increase disease severity.<sup>10</sup> Therefore, broad-spectrum antibiotics should be  
72 considered when selecting effective treatment. Chloramphenicol (CHL) is a broad-spectrum  
73 antibiotic that blocks the peptidyl transferase activity of the bacterial ribosome, which prevents  
74 protein chain elongation and inhibits development growth of bacteria.<sup>11</sup> CHL is effective  
75 against *Enterococcus faecium* in addition to being a broad-spectrum antibiotic, which has led  
76 to its consideration for the treatment of vancomycin-resistant enterococcus.<sup>11,12</sup> However,

77 systemically-administered CHL possesses harmful side effects, such as bone marrow  
78 damage.<sup>11,12,13</sup> This is aggravated by the fact that, due to the rise of antibiotic resistance, CHL  
79 has recently been given to patients in higher doses.<sup>11</sup> Therefore, it is necessary to create and  
80 develop a technique for selective drug administration that can prevent the exposure of CHL to  
81 unwanted sites.

82 Numerous attempts have been previously reported to address this specific problem.  
83 Antibiotic delivery, in particular, can be modified by increasing targeting efficiency or reacting  
84 to environmental triggers, such as enzyme, pH, or temperature<sup>14</sup>. Natural polymers such as  
85 chitosan, cellulose, and albumin are capable of showing both thermal and pH responsive  
86 properties, rendering their vast application for drug delivery<sup>15</sup>. However, precise drug release  
87 still cannot be completely achieved with these polymers, since the biological pH and  
88 temperature fluctuate within a particular range due to individual variances and the degree of  
89 infection<sup>16</sup>. Designing a more precise drug release which can only be induced at a very specific  
90 environmental trigger can become the solution. For instance, it has been reported that  
91 *Staphylococcus aureus* (SA) can produce specifically enzyme like lipolytic esterase. This  
92 enzyme can initiate the biocatalytic hydrolysis of a polymer called polycaprolactone (PCL).<sup>17</sup>  
93 Given this unique property, PCL can be employed as suitable materials to specifically deliver  
94 antimicrobial agents only to the infected tissues. Hence, this approach could prevent exposure  
95 to healthy tissues, resulting in a safer therapeutic approach. One of the utilizations of this  
96 polymer is the formulation of microparticulate or nanoparticulate delivery system.<sup>18</sup> Small  
97 molecules and moderately sized molecules, in the form of micro/nanoparticles, can easily  
98 penetrate both the endothelium of the blood and the lymphatic capillary.<sup>19</sup> Particularly for skin  
99 delivery, microparticles (MPs) have shown to retain drugs better than NPs, and can help  
100 localize long-term drug retention in the skin.<sup>20,21</sup> For that reason, we hypothesize that

101 incorporating chloramphenicol into MPs may enhance their efficiency targeting in skin wound  
102 infections.

103 The effectiveness of the few therapy options for infected wounds is currently limited  
104 by toxicity issues and low-to-moderate eschar penetration concerns. Despite the fact that  
105 bacterial conjunctivitis has previously been treated with chloramphenicol ointment, there are  
106 less data supporting its use in the prevention or treatment of infections in skin wounds.<sup>22</sup>  
107 Chloramphenicol is ineffective for the topical treatment of skin infections due to its  
108 hydrophobic chemical components,<sup>11</sup> which limit effective cutaneous penetration, as human  
109 skin creates an impenetrable barrier that prevents the hydrophobic medication from being  
110 transported that way. The issue becomes more significant in the event of an infected lesion,  
111 when the medicine should penetrate through the skin around infection area and to improve its  
112 therapeutic index.<sup>11</sup> Dissolving microneedles (MNs) are a medication delivery system that may  
113 bypass the primary epidermal barrier.<sup>23</sup> MNs can essentially offer a quick, painless, locally  
114 focused, and patient-compliant administration strategy.<sup>24</sup> Dissolving MNs, in contrast to  
115 hypodermic needle injections, are made of biocompatible polymers and are capable of self-  
116 dissolving. Therefore, their use does not result in the production of biohazardous sharps  
117 waste.<sup>25</sup> Considering the benefits of this technique, adding MPs to dissolving MNs may  
118 enhance the quantity of MPs that reaches the necrotic tissue of infected skin, thereby possibly  
119 improving chronic wound infection management for cellulitis.

120 This study implemented a novel strategy for potentially improving chronic wound  
121 treatment from cellulitis by pioneering the production of MPs loaded with CHL and attached  
122 in dissolving MN system. The MPs were evaluated for their structure, antibacterial properties,  
123 size, and others physicochemical characterization. To examine the effectiveness of MPs in *in*  
124 *vivo* evaluation, we employed the immunodeficient mutant **Drosophila** larval model. The  
125 release behavior of CHL in MPs was specifically tested with and without the presence of

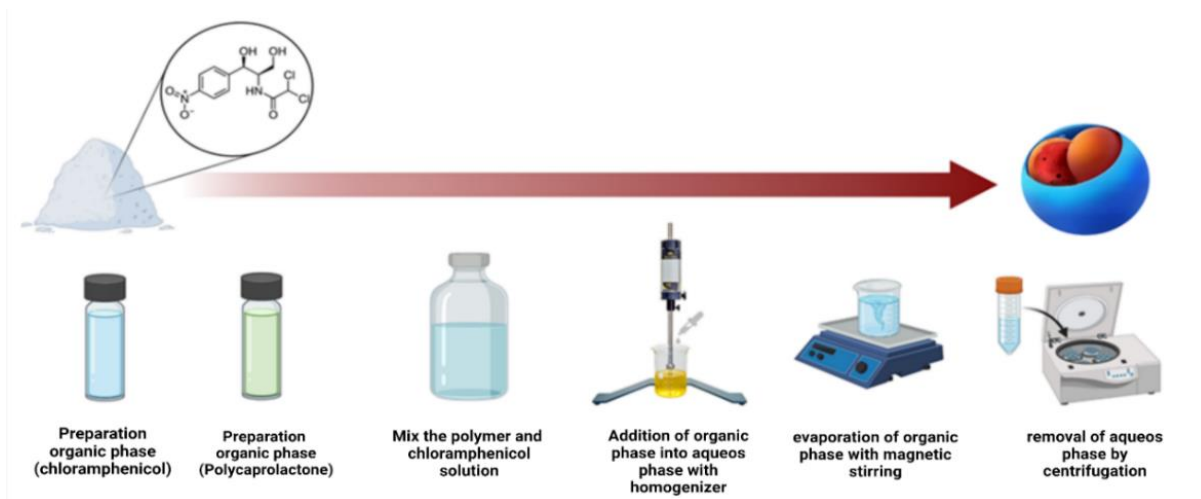
126 microorganisms commonly found in chronic infection wounds of cellulitis. The MPs were then  
127 added to dissolving MNs, which were evaluated for their insertion and mechanical  
128 characteristics. *Ex vivo* infection models in excised infected and normal rat skin were used to  
129 explore the *ex vivo* dermatokinetic characteristics of CHL-loaded MPs. Finally, to assess the  
130 potential effectiveness of this inquiry, an *ex vivo* skin infection model was used to examine the  
131 MPs ability to penetrate and eliminate the burden of bacterial infection.

132

## 133 **2. EXPERIMENTAL SECTION**

134 **2.1. Materials.** Chloramphenicol (CHL) (purity, 100.00%) was purchased from Merck  
135 (Darmstadt, Germany). Polycaprolactone (PCL) (MW 80,000), polyvinyl alcohol (PVA) (MW  
136 9,000–10,000), Polyvinyl pyrrolidone (PVP) (MW 40,000), sodium chloride, Tryptic Soy  
137 Broth (TSB), potassium chloride, disodium phosphate, and potassium dihydrogen phosphate,  
138 were obtained from Sigma-Aldrich (Singapore). All other reagents used were analytical grade.

139 **2.2. Preparation of chloramphenicol sensitive bacterial microparticles (CHL-  
140 Loaded MPs)** Following a previously described procedure with minor modifications, PCL was  
141 used as the polymer and PVA as the surfactant to create CHL microparticles using a solvent-  
142 evaporation approach.<sup>11</sup> Briefly, PCL was dissolved in 7 mL of chloroform and CHL in 3 mL  
143 of methanol. The mixtures were then combined until homogenous. Then, the polymer–drug  
144 mixture was added dropwise into the 25 mL aqueous phase containing 3% PVA as the  
145 hydrophilic surfactant under mechanical homogenizer at 500 rpm for 5 minutes. To ensure the  
146 organic phase evaporated entirely, the emulsion system was left under a magnetic stirrer for  
147 five hours. The MPs were then centrifuged to facilitate collection, rinsed three times with  
148 distilled water, and dried. Figure 1 illustrates the schematic preparation of CHL-loaded MPs.



149

150

**Figure 1.** Schematic illustration of preparation of CHL-loaded MPs.

151

### 2.3. Optimization of **CHL-Loaded MPs** through Experimental Design.

152

Loaded MPs were created using *Design-Expert*<sup>TM</sup> (version 13, Stat-Ease, Inc.) by optimizing

153

the crucial process parameters. Following the response surface methodology and central

154

composite design (CCD), three independent variables can influence the characteristics of the

155

resulting MPs: CHL-PCL ratio (X1), stirring speed (X2), and stirring time (X3). The program

156

carried out 15 runs of formulas for provided values of low and high levels of these factors,

157

denoted by 1 and +1, respectively. These values were also established empirically during pre-

158

formulation screening. For **CHL-Loaded MPs** optimization, dependent variables to be

159

examined included particle size (Y1), polydispersity index (PDI) (Y2), entrapment efficiency

160

(EE%) (Y3), and drug loading (DL%) (Y4). Table 1 displays the composition of 15

161

formulations with the dependent variable outputs.

162

163

164

165 **Table 1.** Composition, characteristics design, and mean of particle size, PDI, entrapment  
 166 efficiency (EE), and drug loading (DL), of **CHL-loaded MPs**

Run	Independent Variables			Dependent Variables			
	X1	X2 (rpm)	X3 (minutes)	Y1 ( $\mu\text{m}$ )	Y2	Y3 (%)	Y4 (%)
<b>F1</b>	1	500	15	17.96	0.022	41.54	22.77
<b>F2</b>	1	1000	10	16.40	0.018	32.74	16.37
<b>F3</b>	15	500	15	59.46	0.030	50.82	3.17
<b>F4</b>	1	1500	5	7.38	0.010	38.76	19.38
<b>F5</b>	8	1000	10	49.04	0.009	44.69	4.96
<b>F6</b>	8	1500	10	30.34	0.010	44.31	4.92
<b>F7</b>	15	1000	10	58.85	0.012	49.10	3.06
<b>F8</b>	8	1000	15	38.41	0.004	37.42	4.15
<b>F9</b>	1	1500	15	5.82	0.389	34.55	17.27
<b>F10</b>	1	500	5	22.37	0.010	44.41	22.20
<b>F11</b>	8	1000	5	54.53	0.008	44.98	4.99
<b>F12</b>	15	1500	5	55.13	0.005	49.19	3.07
<b>F13</b>	15	1500	15	47.10	0.007	45.46	2.84
<b>F14</b>	8	500	10	58.68	0.012	45.56	5.06
<b>F15</b>	15	500	5	71.26	0.013	55.70	3.48

167  
 168 **2.4. Characterization of CHL-loaded MPs.** The diameter and polydispersity index  
 169 (PDI) of CHL-loaded MPs were determined using a microscope (Olympus CS33, Olympus  
 170 Corporation) and was calibrated using a 10x magnification Optilab<sup>®</sup> camera. Zeta potential of  
 171 CHL-loaded MPs was determined using zeta potential analyzer (Brookhaven, New York,  
 172 USA)

173 An indirect technique was used to measure the EE of CHL in the MPs formulations.<sup>26</sup>  
 174 After three washing cycles, the free CHL concentration in the supernatant was measured using

175 spectrophotometry UV-VIS (Dynamica, HALO XB-10, Dynamica Scientific Ltd, UK).

176 Finally, equation (1) was used to determine the EE of CHL.

177 
$$EE\% = \frac{\text{Drug Total}-\text{Drug Free}}{\text{Drug Total}} \times 100\% \text{ (Equation 1)}$$

178 To determine the DL percentage of CHL in MPs formulations, 10 mg of dried MPs was  
179 dispersed into a 7:3 methanol: chloroform mixture, which was placed in sonicator for one hour  
180 to disrupt the MP matrix. Following a 15-minute centrifugation at 14,000 rpm of the  
181 suspension, the concentration of CHL in the supernatant was determined using a  
182 spectrophotometer UV-VIS (Dynamica, HALO XB-10, Dynamica Scientific Ltd, UK).

183 Equation (2) was used to calculate the DL percentage.

184 
$$DL\% = \frac{\text{Amount of Encapsulated CHL}}{\text{Total Weight}} \times 100\% \text{ (Equation 2)}$$

185 A scanning electron microscope (SEM) was used to examine the morphologies of the  
186 CHL-loaded MPs (Hitachi, Krefeld, Germany). A Fourier transform infrared (FTIR)  
187 spectrometer (Accutrac FT/IR-4100TM Series, Jasco, Essex, UK) was used to examine the  
188 chemical interactions between each component in the formulas. A differential scanning  
189 calorimeter was used to conduct thermal profile investigation of CHL, polymers, physical  
190 mixtures, and CHL-loaded MPs (DSC 2920, TA Instruments, Surrey, UK). An X-ray  
191 diffractometer instrument was used to perform crystalline profile diffraction on CHL and CHL-  
192 loaded MPs (Rigaku Corporation, Kent, England).

193 **2.5. Hemolytic activity of CHL-loaded MPs.** In this investigation, the hemolysis  
194 potential of the cells may be utilized to evaluate the biocompatibility and safety of the designed  
195 drug delivery system. Following a previously described procedure, an *in vitro* hemolytic  
196 experiment was carried out to evaluate the hemolytic activity of CHL-Loaded MPs.<sup>27</sup> Briefly,  
197 erythrocytes were collected from the blood of healthy female Sprague–Dawley rat by  
198 centrifugation at 2000 RCF for 10 minutes. The blood was then washed with PBS and

199 processed to three cycles of centrifugation under the same conditions. The erythrocytes were  
200 washed and resuspended in PBS to a final concentration of 10% v/v. In 900  $\mu$ L of samples  
201 containing CHL and CHL-loaded MPs diluted in PBS until they reached 5, 50, and 500  $\mu$ g/mL  
202 concentrations. Then, 100  $\mu$ L of the produced cell (erythrocytes) suspension was added. After  
203 that, the mixtures were centrifuged at 14,000 RCF for 10 minutes after being incubated at 37°C  
204 for 60 minutes. Finally, to determine the amount of free hemoglobin, UV-visible spectroscopy  
205 was used to measure the absorbance of the supernatant (Dynamica, HALO XB-10).  
206 Accordingly, PBS and distilled water were used as negative and positive hemolytic controls.  
207 To assess the hemolysis of the samples, a change in the color of sample mixture was also seen.  
208 For each concentration, the experiment was run in three replications. Equation (3) was used to  
209 determine the hemolysis percentage:

$$210 \quad \text{Hemolysis (\%)} = \frac{\text{OD (Test Sample)} - \text{OD (Negative control)}}{\text{OD (Positive control)} - \text{OD (Negative control)}} \times 100\% \text{ (Equation 3)}$$

## 211 ***2.6. In-vitro antibacterial activities***

212 ***2.6.1. Culture of bacterial strains.*** The microorganism employed in this investigation  
213 was SA ATCC 25923. The strains were purchased from LGC Standards in Middlesex, UK,  
214 kept at 4°C, and were sub-cultured on new media at regular intervals. Before each antibacterial  
215 experiment, the bacterial strains were cultured overnight and incubated at 37°C in TSB media.  
216 Serial dilutions with TSB were used to create inoculums of bacteria (placing the diluted mixture  
217 on tryptic soy agar (TSA) plates allowed for the accurate counting of bacteria), resulting in  
218 final concentrations of  $1.5 \times 10^8$  colony forming units (CFU)/mL.

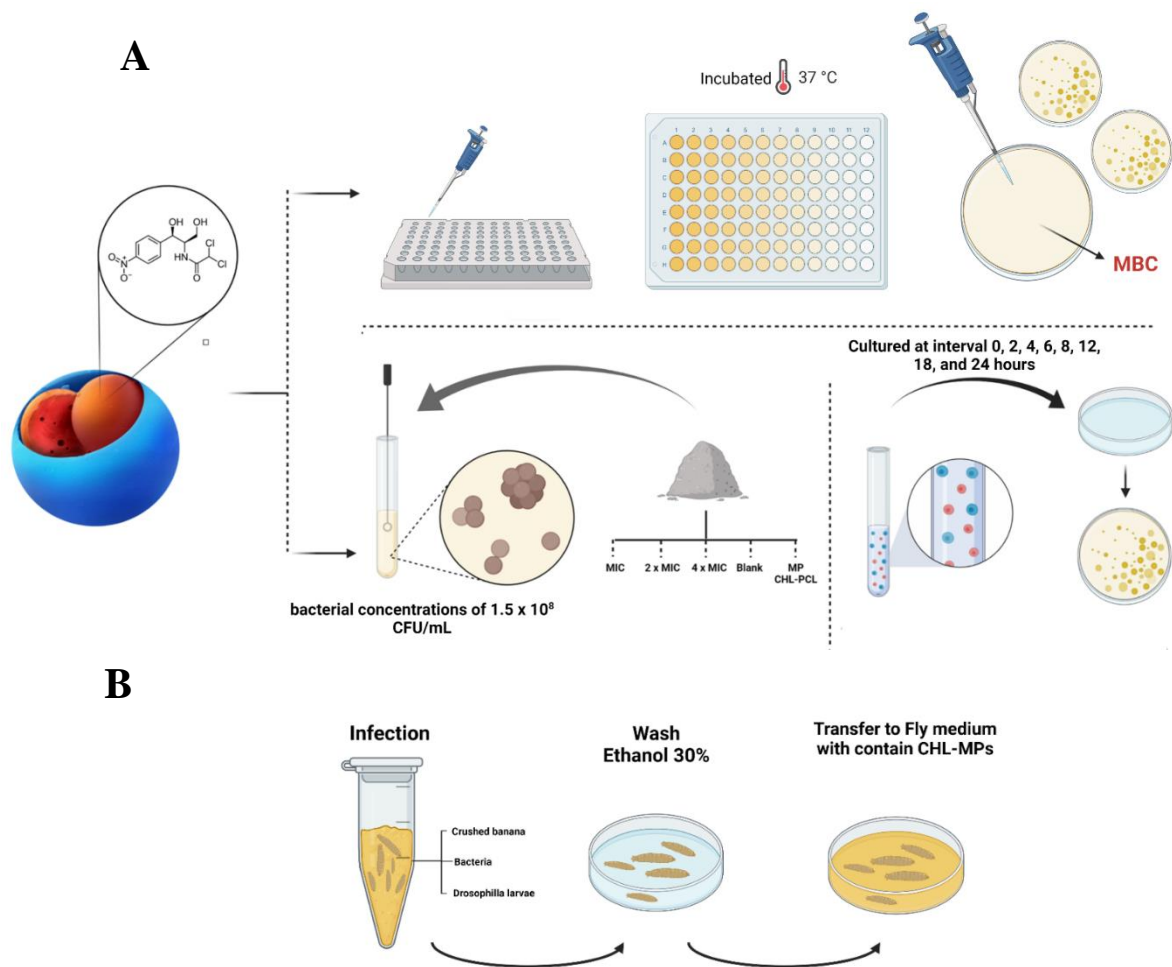
219 ***2.6.2. Determination of minimum inhibitory concentration and minimum***  
220 ***bactericidal concentration.*** As previously described, a microtiter broth dilution technique was  
221 used to determine the minimal inhibitory concentrations (MICs) and minimal bactericidal

222 concentrations (MBCs) of CHL and CHL-loaded MPs in 96 well bottom plates.<sup>28</sup> Various  
223 concentrations of CHL and CHL-loaded MPs (3.125–200 µg/mL) were used to calculate the  
224 MIC in TSB along with the corresponding equilibrated concentrations of chloramphenicol.  
225 Each tube received a 100 µL volume of each bacterial inoculum, which was then cultured for  
226 24 hours at room temperature (See Figure 2a). The positive and negative controls utilized were  
227 TSB and TSB with bacteria, respectively. The lowest concentration of the tested substance,  
228 which had no visible growth after 24 hours of incubation, was considered the MIC.

229 MBC was calculated by cultivating 20 µl on TSA plates and incubating them at 37°C  
230 for 24 hours in wells corresponding to the MIC and the above-mentioned dilutions. The  
231 researchers then determined how many bacterial colonies were present on the plates. The MBC  
232 was determined to be the lowest concentration that inhibited 99.9% of bacterial growth.  
233 Equation (4) was used to determine the killing percentage

234 
$$\text{Killing percentage (\%)} = \frac{\text{CFU (Control)} - \text{CFU (experiment)}}{\text{CFU (Control)}} \times 100\% \text{ (Equation 4)}$$

235 **2.6.3. Time kill assay.** Following the procedure outlined before described, the time-  
236 killing kinetics of CHL and CHL-loaded MPs against SA was determined.<sup>29</sup> MPs loaded with  
237 CHL were created and added to the bacterial suspensions ( $1.5 \times 10^8$  CFU/mL). CHL doses  
238 corresponding to MIC, 2x MIC, and 4x MIC were also prepared and applied. Then, 37°C of  
239 incubation was applied to the bacterial cultures. 20 µl aliquots from the cultures were obtained  
240 at intervals of 0, 2, 4, 6, 8, 12, 18, and 24 hours and aseptically injected on TSA plates. To  
241 calculate the bacteria's viable CFU, the plates were incubated for 24 hours at 37°C. The  
242 procedure was performed in triplicate, and a log CFU/mL vs time kill curve was constructed.  
243 Figure 2a illustrates the schematic time kill assay.



244

245

246

247

## 2.7. *In vivo* antibacterial activities in *Drosophila* larval model

248

### 2.7.1. *Bacterial strains and fly stocks.* SA ATCC 25923 was the bacterial strain used

249

as the infecting agent. It was purchased from LGC Standards in Middlesex, UK, and kept at

250

4°C. Bacteria were cultivated separately in TSB medium and incubated at 37°C. When the

251

cultures had grown to their maximum potential, they were collected, rinsed with PBS, and

252

employed in the tests. This study used the psh [1];;modSP[KO] *Drosophila* line, which is an

253

immunodeficient fly line that lacks toll pathway activity. All flies were kept on conventional

254

cornmeal-agar medium at a temperature of 25°C.

255           **2.7.2. Infection experiment.** The infection experiment on larval *Drosophila* was carried  
256 out as previously described with minor modifications.<sup>30</sup> Two and a half days after egg laying,  
257 the researchers began infecting mid-L2 larvae. Animals were put in a 1.5 mL microcentrifuge  
258 tube for 30 minutes per test, along with 300 µl of crushed bananas and 300 µl of an overnight  
259 bacterial culture (See Figure 2b). A foam stopper was used to obstruct the animals, ensuring  
260 that they stayed at the bottom of the tube for the duration of the infection. Upon completion of  
261 this stage, they were quickly cleaned in 30% ethanol before being put on a petri dish with a  
262 new fly medium free of yeast and containing CHL-loaded MPs. Waiting durations and  
263 infections were conducted at 29°C.

264           **2.8. In-vitro release study of CHL-loaded MPs in bacterial cultures.** **The in vitro**  
265 **release study of CHL-loaded MPs in bacterial cultures was determined.** The release tests of  
266 CHL and CHL-loaded MPs were carried out in presence or absence of bacteria in fluid  
267 mimicking infection media.<sup>17</sup> Briefly, MPs with a CHL equivalent of 50 mg were dissolved in  
268 50 mL of the bacterial cultures and incubated at 37°C and 100 rpm in an orbital shaker. At  
269 0.25, 0.5, 0.75, 1, 2, 3, 4, 5, 6, 7, 8, and 24 hours of incubation, samples from the cultures were  
270 taken out and inoculated on TSA plates with the proper dilutions. At predetermined intervals,  
271 0.5 mL aliquots of the sample were removed and filtered. The concentration of CHL in the  
272 filtrate was measured using a spectrophotometer UV-VIS.

273           To assess the kinetic release profiles, DDSolver (China Pharmaceutical University,  
274 Nanjing, China),<sup>31</sup> was used to fit in Five mathematical models like, zero-order kinetics (ZO),  
275 first-order kinetics (FO), Higuchi model, Korsmeyer–Peppas (KP), and Hixson–Crowell (HC).

276

277

278 Zero Order Kinetics :  $C_t = C_0 + k_0 t$  (Equation 5)

279 First Order Kinetics :  $\ln C_t = \ln C_0 + k_1 t$  (Equation 6)

280 Higuchi Model :  $C_t = k_H \sqrt{t}$  (Equation 7)

281 Korsmeyer-Peppas Model :  $C_t = k_{KP} t^n$  (Equation 8)

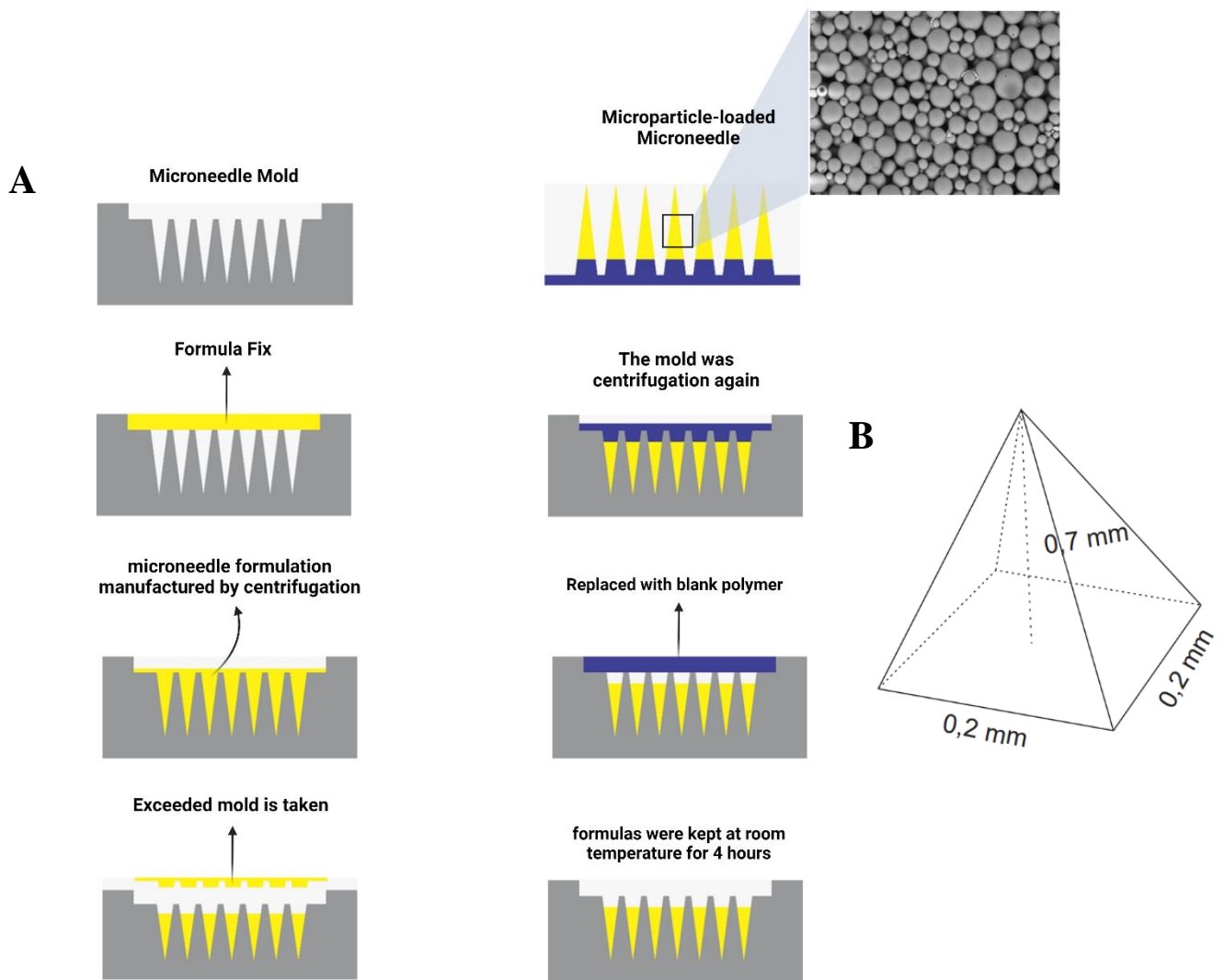
282 Hixson-Crowell Model :  $C_t^{1/3} = C_0^{1/3} + k_{HC} t$  (Equation 9)

283  $C_t$  denotes the concentration of CHL at period  $t$ ,  $C_0$  indicates a primary combination  
284 of CHL in-side of medium ( $t=0$ ),  $K_0$ ,  $K_1$ ,  $K_H$ ,  $K_P$ , and  $K_{HC}$  were the coefficients of release  
285 of the relevant kinetic models. A calculation from every type will be explained and the fit of  
286 release kinetics was selected by a reciprocity of coefficient ( $r^2$ ).

287 **2.9. Formulation Design and Manufacture of CHL-MPs loaded Dissolving**  
288 **Microneedle (MNs).** A two-step manufacturing procedure was used to create two-layered  
289 dissolving MNs, with a few minor modifications.<sup>20,25</sup> The polymer solutions were mixed with  
290 the ratio depicted in Table 2. The same quantity of CHL-loaded MPs pellets was combined  
291 with the polymer mixture to create the MNs formulation. They were then exposed to sonication  
292 to achieve a clean bubble-free dispersion. Then, 50 mg of the mixture was poured into the  
293 silicone MN molds. The polymer–drug combination was then put on the mold and centrifuged.  
294 Following centrifugation, the extra polymer mixture at the top of the mold was extracted and  
295 replaced using a spatula; the formulas were kept at room temperature for 4 hours. Following  
296 that, the two-layered MNs were created by pouring an aqueous gel containing blank polymer  
297 mixtures. Then, the molds were centrifuged again. The produced MNs were then dried for 24  
298 hours at room temperature and 24 hours at 37°C without being removed from the mold (See  
299 Figure 3). In addition to MNs with CHL-loaded MPs, MNs with free CHL were generated for  
300 additional research using the same procedure. Figure 3 is schematic illustration of  
301 manufacturing the two-layered MNs.

**Table 2** Composition of formulations MNs containing CHL-loaded MPs

<b>Formulas</b>	<b>Concentration (%b/b)</b>			
	MPs	PVP	PVA	Aquadest
<b>F1</b>	25	20	15	40
<b>F2</b>	25	20	20	35
<b>F3</b>	25	20	25	30
<b>F4</b>	25	25	20	30
<b>F5</b>	25	15	20	40



304

305 **Figure 3.** Two-layer dissolving MNs manufacturing scheme (A), MNs dimensions (B).

306 **2.10. Mechanical strength and penetration ability test.** To assess the MNs response  
 307 after applied pressure, mechanical strength and penetrating ability tests were carried out using  
 308 the previously stated approach with minor modifications.<sup>32</sup> This assessment was done by  
 309 measuring the MNs capacity penetration through eight layers of parafilm®, which was the  
 310 same thickness as the top layer of human skin. Pressure (30 N) was used to apply the MNs for  
 311 30 seconds. A weight of 3.06 kg was placed on top of the microneedles to create this pressure.  
 312 It is important to note that during the trial, equal pressure was applied to all sides of the MNs.  
 313 Then, the number of holes in each layer of parafilm® was counted and MNs size and shape

314 were examined under a microscope in accordance with technique described previously.<sup>33</sup> The  
315 following calculations are used to compute the proportion of mechanical strength and MNs  
316 penetration capability.<sup>34</sup>

$$317 \quad \text{compression \%} = \frac{\text{initial height} - \text{height after pressure applied}}{\text{initial height}} \times 100\% \quad (\text{Equation 10})$$

$$318 \quad \% \text{ penetration of n layer} = \frac{\text{Number of holes in n layer}}{\text{total number of holes}} \times 100\% \quad (\text{Equation 11})$$

319 **2.11. Calculation of drug content localized to the needles.** To quantify the amount of  
320 CHL in MNs, needle MNs were scraped carefully from the baseplate using a scalpel and then  
321 dissolved in 5 mL of distilled water. Methanol : chloroform mixture with ratio of 7 : 3 (2 ml)  
322 was added to the dispersion and placed in sonicator for one hour to disrupt the MP matrix.  
323 Following a 15-minute centrifugation at 14,000 rpm of the suspension, the concentration of  
324 CHL in the supernatant was determined using a spectrophotometer UV-VIS (Dynamica,  
325 HALO XB-10, Dynamica Scientific Ltd, UK)

326 **2.12. Stability Test of MPs-CHL loaded into MNs.** MNs containing CHL-loaded MPs  
327 were kept in static storage at 25°C. The initial sizes, PDIs, EE, DL, and zeta potentials were  
328 compared to those obtained in 10 days and storage at 25°C to determine stability. The statistical  
329 analysis was used to assess the significance stability of MPs.

330 **2.13. Dissolution study, ex vivo dermatokinetic studies and anti-infection activity in**  
331 **ex vivo model of infection on rat skin**

332 **2.13.1. Preparation of ex vivo model of infection on rat skin.** Wistar rats' abdomen  
333 skins were removed and placed in PBS before the experiment (pH 7.4). Rat skins were washed  
334 in ethanol at a 70% concentration for one hour. The skins were kept in a biosafety cabinet for  
335 20 minutes to allow the ethanol to evaporate before wounding the surface 5 mm with a biopsy  
336 punch (Stiefel, Middlesex, UK). The previously reported procedures were then applied to

337 develop *ex vivo* models of infection on rat skin, with a few minor modifications.<sup>35</sup> After  
338 wounding and infection, the skins were transferred on TSA plates and 50  $\mu$ L of the diluted  
339 bacterial suspension ( $1.5 \times 10^8$  CFU/mL) were equally injected to the wound of the skin. Every  
340 day for five days, the skins were moved to new TSA media plates, which were then incubated  
341 at 37°C to encourage the formation of the infection.

342 **2.13.2. Dissolution study.** The MNs dissolution study was assessed in an *ex vivo* model  
343 of skin infection. Briefly, the MN arrays were physically implanted into the epidermal area,  
344 and a 5.0 g cylindrical stainless-steel weight was placed on top to guarantee the array stayed in  
345 place. MN arrays were collected at various interval time points and examined using a Leica  
346 EZ4 D stereo microscope.

347 **2.13.3. Ex vivo dermatokinetic studies.** *Ex vivo* dermatokinetic tests of MNs containing  
348 free CHL and CHL-loaded MPs were performed on excised full-thickness skin in both infected  
349 and infection models. This investigation was conducted using the previously outlined  
350 methodology.<sup>23,25</sup> Initially, cyanoacrylate glue was used to affix the skin to the franz cell  
351 diffusion cells' donor compartment. The receiver chamber with PBS was coupled with another  
352 donor compartment., and the MNs were manually forced into the skin for 30 seconds (pH 7.4).  
353 The MNs were kept in place during the experiment by a cylindrical stainless steel mass that  
354 weighed 5 g. The recipient compartment's temperature was maintained at  $37 \pm 1^\circ\text{C}$ , and  
355 Parafilm<sup>®</sup> was employed to seal the donor compartment and sampling side. At 600 rpm, the  
356 compartment was agitated. At regular intervals (1, 2, 3, 4, 5, 6, 8, and 24 h), the MNs were  
357 taken, and the skin was then three times washed with sterile water. To extract the CHL released  
358 in the skin, the skin sample was then collected and the surface was cleaned with distilled water.  
359 After cleaning, the skin sample was cut into small pieces and 2 ml of PBS was added to extract  
360 CHL from the tissue. The sample was then vortexed for 5 minutes and centrifuged at 14,000

361 rpm for 15 minutes. The supernatant was analyzed using a UV-VIS spectrophotometer  
362 instrument (Dynamica, HALO XB-10, Dynamica Scientific Ltd, UK).

363 To assess the dermatokinetic profiles, PKSolver (China Pharmaceutical University,  
364 Nanjing, China),<sup>31</sup> was used in a one-compartment open model. We calculated the drug  
365 concentration time curve from time zero (t=0) to the end experimental time point (t=24 h)  
366 (AUC), the mean half-life (t<sub>1/2</sub>), the mean residence time (MRT), the maximum drug  
367 concentration in skin (C<sub>max</sub>), and the time of maximum concentration (t<sub>max</sub>). To ensure that  
368 the skin extraction method was only able to remove the CHL released from MPs without  
369 harming the MPs, the extraction method was applied to the CHL-loaded MPs dispersion, and  
370 processed using the same steps. It should be noted that the extraction method did not affect the  
371 CHL encapsulated in the MPs. Comparative investigations were carried out utilizing MPs that  
372 were loaded with specific amounts of CHL and needle-free patches conveying free CHL.

373 **2.13.4. Antimicrobial activity in ex vivo model of infection on rat skin.** The technique  
374 previously described,<sup>35,36</sup> was used to measure anti-infection activity, with a few minor  
375 modifications. 20 µL of the supernatant from dermatokinetic experiments 24 and 48 hours after  
376 application time was inoculated onto TSA plates and was incubated for 24 hours at 37°C to  
377 assess the anti-infection effectiveness of MNs formulation loaded with CHL and MPs-CHL in  
378 an *ex vivo* model. Additionally, the same procedure was carried out using cream containing  
379 CHL and CHL-loaded MPs on the diseased skin. Finally, the number of viable CFU was  
380 determined. Normal skin was utilized as a negative control, while infected skin was used as a  
381 positive control without MNs treatment.

382 **2.14. Statistical analysis.** The findings of the experiment were presented as means and  
383 standard deviations (SD) of the means. GraphPad Prism<sup>®</sup> version 6 was used (GraphPad  
384 Software, San Diego, California, USA) for statistical analysis. An unpaired t-test was employed

385 to compare the two groups. In addition, the Kruskal–Wallis test with a post-hoc Dunn’s test  
386 was utilized to compare different groups. Statistical significance is indicated by a value of  
387  $p < 0.05$ .

### 388 **3. Results and Discussion**

389 **3.1. Formulation of CHL-loaded MPs.** The solvent-evaporation approach was used to  
390 prepare CHL–loaded MPs, because this approach is suitable for producing MPs containing  
391 hydrophobic compounds such as CHL.<sup>11</sup> The initial issue was choosing an organic phase that  
392 could dissolve both chloramphenicol and the polyester polymer, PCL. A mixture of methanol  
393 and chloroform solvent with a ratio of 7: 3 was used to create CHL-Loaded MPs because these  
394 solvents mixed well and homogenously (i.e.,clear), and no harmful chlorinated organic  
395 solvents were used to incorporate the drug into the MPs. The cosolvent was also employed to  
396 aid in the solubility of CHL, which was then integrated into the hydrophobic core of CHL-  
397 loaded MPs.

398 **3.2. Statistical analysis of experimental data by Design-Expert software.** A total of 15  
399 formulations with various level of ratio CHL: PCL (X1), stirring speed (X2), and stirring time  
400 (X3) were successfully formulated and screened using CCD under Design-Expert™ (version  
401 13, Stat-Ease, Inc, Minneapolis, USA). The best mathematical model was selected based on  
402 statistical goodness-of-fit including F-value, predicted and adjusted R-squared values, and  
403 adequate precision. After confirming the model significance in terms of an analysis of variance  
404 test with a  $p$ -value of 0.05 or below, the data were evaluated. The impact of each independent  
405 variable on different answers was calculated after critical analysis.

406 **3.2.1. Effect of independent variables on particle size.** The physicochemical  
407 characteristics (e.g., drug loading, release profile, bioavailability) and physiological behavior  
408 (e.g., interaction with plasma components, phagocytosis, uptake) of MPs are commonly

409 dependent on particle size.<sup>37</sup> The 15 formulations tested in this study had mean particle sizes  
410 between 5.82 and 71.26  $\mu\text{m}$  (Table 1), which is ideal for skin penetration and retention.<sup>20</sup>  
411 Compared to the quadratic and two-factor models, the linear model, with an R-squared value  
412 of 0.9196 and an adjusted R-squared value of 0.8976, was determined to be the best match for  
413 answer Y1. ANOVA was used to assess the linear model's significance for the quantitative  
414 impacts of variables on response. The linear model had a significant ANOVA result ( $p < 0.05$ )  
415 and a model F-value of 41.92. The signal to noise ratio is measured by "Adeq Precision," and  
416 a value greater than 4 is preferred.<sup>38</sup> The calculated ratio, 19.827, suggested that the anticipated  
417 model would be helpful in guiding the design space. An empirical polynomial equation based  
418 on data analysis was produced and is represented by the following coded factors:

419 ***Mean particle size ( $\mu\text{m}$ )***

420 
$$Y1 = + 39.34292 + 3.16933X1 - 0.016791X2 - 0.838608X3 \text{ (Equation 12)}$$

421 Regarding the ANOVA results, CHL:PCL Ratio (X1) and stirring speed (X2) had a  
422 significant impact on particle size. According to Equation (12), the significant positive  
423 coefficient for X1 indicated that the particle size significantly increased with increasing  
424 polymer concentration ( $p < 0.05$ ). This can be explained by the fact that when polymers are  
425 more highly concentrated, there are more interactions between particles during emulsification.  
426 This causes the fusing of partially formed particles, which in turn causes an increase in particle  
427 size.<sup>39</sup> Additionally, increasing polymer content increases the organic phase's viscosity, which  
428 finally slows down its diffusion into the aqueous phase and produces bigger microparticles.<sup>40</sup>  
429 Further, the significant negative coefficient for X2 indicated that the particle size significantly  
430 decreased with increasing stirring speed ( $p < 0.05$ ). This is because emulsification at fast speed  
431 can lead to a reduction in emulsion globules; as a result, a lower emulsion globule size  
432 permitted the production of smaller microparticles. As homogenization proceeds more quickly,

433 more energy is released, which causes the polymeric organic phase to disperse more quickly  
434 and produces small microparticles with monomodal distributions. The values of the X2 and X3  
435 coefficients were negative, indicating an inversely proportional effect with the resulting  
436 particle size response. However, stirring time coefficients for X3 were not significant  
437 ( $p > 0.05$ ).

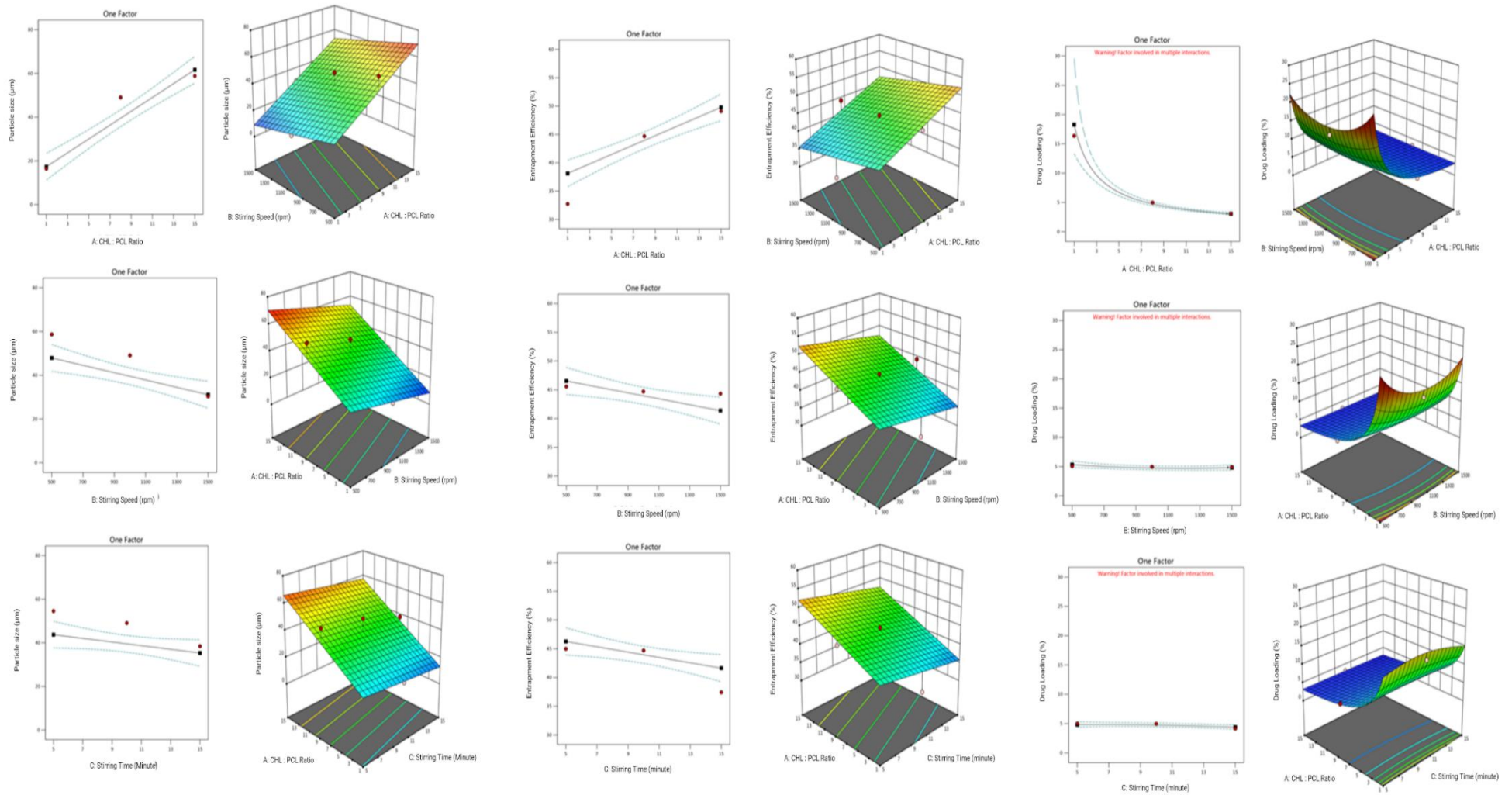
438         Two variables can have simultaneous impacts, which can be shown in 3D surface plots.  
439 Plot X1X2's curved shape showed that the factors strongly interacted to affect particle size.  
440 Although CHL:PCL ratio and stirring speed are clearly correlated to particle size, these  
441 relationships are not statistically significant ( $p > 0.05$ ) based the positive coefficient value for  
442 stirring time (X3). As seen in Figure 4A, two and three dimensional surface plots vividly  
443 demonstrate how numerous independent factors affect particle size. The intensity of the red  
444 hue indicates an increase in particle size with corresponding changes CHL:PCL ratio, stirring  
445 speed, and stirring time

446

447

448

449



450

451

**Figure 4.** 2D and 3D response surface graphs displaying the impact of independent factors on particle size (A), EE% (B), and DL% (C).



473 According to the ANOVA results, the linear coefficients (X1, X2, and X3) with p-values  
474 0.05 substantially impacted the EE percentage. The positive coefficient for X1 in Equation (13)  
475 demonstrates that as the concentration of hydrophobic polymer increases, EE increases ( $p < 0.05$ ),  
476 which may be explained by the hydrophobicity of CHL and its higher miscibility in the organic  
477 phase. Previous research has noted this pattern for hydrophobic medicines, indicating that enhanced  
478 interactions with polymeric solutions and increased organic phase consistency diminish drug  
479 partitioning in the aqueous phase, leading to higher MPs encapsulation.<sup>41</sup>

480 Regarding the other parameter coefficient, the negative coefficient for X2 dan X3 indicated  
481 that entrapment efficiency significantly increased with decreased parameter speed and time of  
482 Stirring ( $p < 0.05$ ). This may be due to the higher speed and longer time of homogenization; more  
483 energy is released in the process that leads to a rapid dispersion of polymeric organic phase. As a  
484 result, the entrapment process becomes shorter, and more drug is released in the polymer matrix,  
485 thereby reducing the entrapment efficiency. Surface graphs in two and three dimensions clearly  
486 show how different independent factors affect the EE% (Figure 4B). The intensity of the red hue  
487 corresponds to an increase in the EE% with the corresponding changes in changes of CHL: PCL  
488 ratio, stirring speed, and stirring time.

489 **3.2.4. Effect of independent variables on DL percentage.** DL is the process of incorporation  
490 of drug into a carrier system. The DL percentage for CHL, which varied from 2.84 to 22.77%, is  
491 shown in Table 1. In comparison to linear and two-factor models, a quadratic model with R-squared  
492 of 0.9971 and an adjusted R-squared of 0.9918 was found to be the best fit for answer Y4 (DL).  
493 According to the ANOVA test, the quadratic model is significant ( $p < 0.05$ ), and the model's F-  
494 value is 190.29, implying that there is only a 0.01% chance of error. Additionally, a low CV value  
495 of 5.37% made it abundantly evident that the experimental results had a high degree of

496 dependability and accuracy. Adeq Precision is parameter that measures the signal to noise ratio. A  
497 ratio greater than 4 is desirable. This study obtained a ratio of 36.367, indicating adequate signal  
498 and showing that the expected model was very useful for traversing the design space. Based on data  
499 analysis, the final equation is shown below.

500 ***Drug Loading (%)***

501 
$$\frac{1}{Y_4} = + 0.000729 + 0.021958X_1 + 0.000104X_2 - 0.005387X_3 - 0.000402 X_1^2$$
 (Equation 14)

502 According to the ANOVA results, the CHL:PCL ratio (X1), stirring speed (X2), and stirring  
503 time (X3), and the polynomial models of CHL: PCL ratio (X1<sup>2</sup>) were significant ( $p < 0.05$ ).  
504 However, the remaining term coefficients were not significant ( $p > 0.05$ ). Based on Equation (14),  
505 the positive coefficient for X1 is associated with the 1/Y4 value indicating that the drug loading  
506 decreased significantly with increasing CHL:PCL ratio ( $p < 0.05$ ). this phenomenon is the same as  
507 previously described regarding the entrapment efficiency by the hydrophobicity of CHL and higher  
508 miscibility in the organic phase. Thus, the enhanced interaction with the polymer solution and the  
509 increased consistency of the organic phase reduced drug partitioning in the aqueous phase, leading  
510 to higher MP encapsulation. However, the increase in the CHL:PCL ratio will increase the weight  
511 of the microparticles, thereby also decreasing the DL value.

512 The positive coefficient for X2 when associated with variable 1/Y4 values indicates that  
513 drug loading decreases significantly with increasing stirring speed ( $p < 0.05$ ). This phenomenon is  
514 similar to the one previously described. This may be due to the higher speed and longer  
515 homogenization time; more energy is released in the process, which leads to the fast dispersion of  
516 the polymer organic phase. As a result, the entrapment process becomes shorter, and more drug is  
517 released into the polymer matrix, thereby reducing the entrapment efficiency and resulting in a

518 reduced DL value. However, this is different from the X3 parameter. The negative coefficient for  
519 X3 when associated with variable values indicates that drug loading increases significantly with  
520 longer stirring time ( $p < 0.05$ ). Surface graphs in two and three dimensions clearly show how  
521 different independent factors affect the DL% (Figure 4C). The intensity of the red hue corresponds  
522 to an increase in the DL% with the corresponding changes in changes CHL:PCL ratio, stirring  
523 speed, and stirring time.

524 **3.3. Optimization and validation.** Following analysis of polynomial equations with  
525 independent and dependent variables, additional optimization and validation were performed. The  
526 optimal formula solution for CHL-loaded MPs creation with desired properties was obtained for  
527 this purpose by using design expert software (minimum for particle size and PDI and maximum for  
528 EE and DL). The improved formulation had a 1:1 of CHL to PCL, a stirring speed of 500 rpm, and  
529 5 minutes of stirring time. The projected values of particle size (Y1), polydispersity index (PDI)  
530 (Y2), entrapment efficiency (EE%) (Y3), and drug loading (DL%) (Y4) at these levels were 29.697,  
531 0.012, 42.955, and 23.283, respectively. These values had a desirability of 0.647 (i.e., having a  
532 64.7% chance of producing the predicted results in terms of dependent variable). CHL-loaded MPs  
533 were then created using the recommended ideal values, and the projected model's accuracy was  
534 checked. The validity of the CCD used to generate the necessary CHL-loaded MPs formulation was  
535 proven by the minimal variance between theoretical predictions and actual outcomes.

536 **3.4. Physicochemical characterization of optimized MP CHL-PCL formulation.** The  
537 breadth of the size distribution and subsequent medication penetration through the skin are  
538 determined by both particle size and PDI. The predicted and observed response variables of the  
539 optimal manufacturing CHL-loaded MPs can be seen in Table 3. The 24.33  $\mu\text{m}$  particle size of the  
540 optimized CHL-loaded MPs formulation was consistent with the expected value (28.595  $\mu\text{m}$ ). The

541 0.010 PDI value obtained was also consistent with the expected value (0.011), showing that the  
 542 formulations were monodisperse and homogenous. Figure 5D shows the morphologies of CHL-  
 543 loaded MPs as seen by SEM. SEM scans revealed that all formulations had spherical shapes.  
 544 Regarding the other parameters, the most crucial factors affecting MPs' desired therapeutic action  
 545 were entrapment efficiency and drug loading. EE and DL percentages of 40.96 and 20.48%,  
 546 respectively were displayed by optimized CHL-loaded MPs, which were close to the expected  
 547 values of 42.61 (EE) and 21.53% (DL). Based on the validation findings, the results align with the  
 548 predicted value with a bias level below of 15%.

549 **Table 3.** Predicted and observed response variables of the optimal manufacturing CHL-Loaded  
 550 MPs

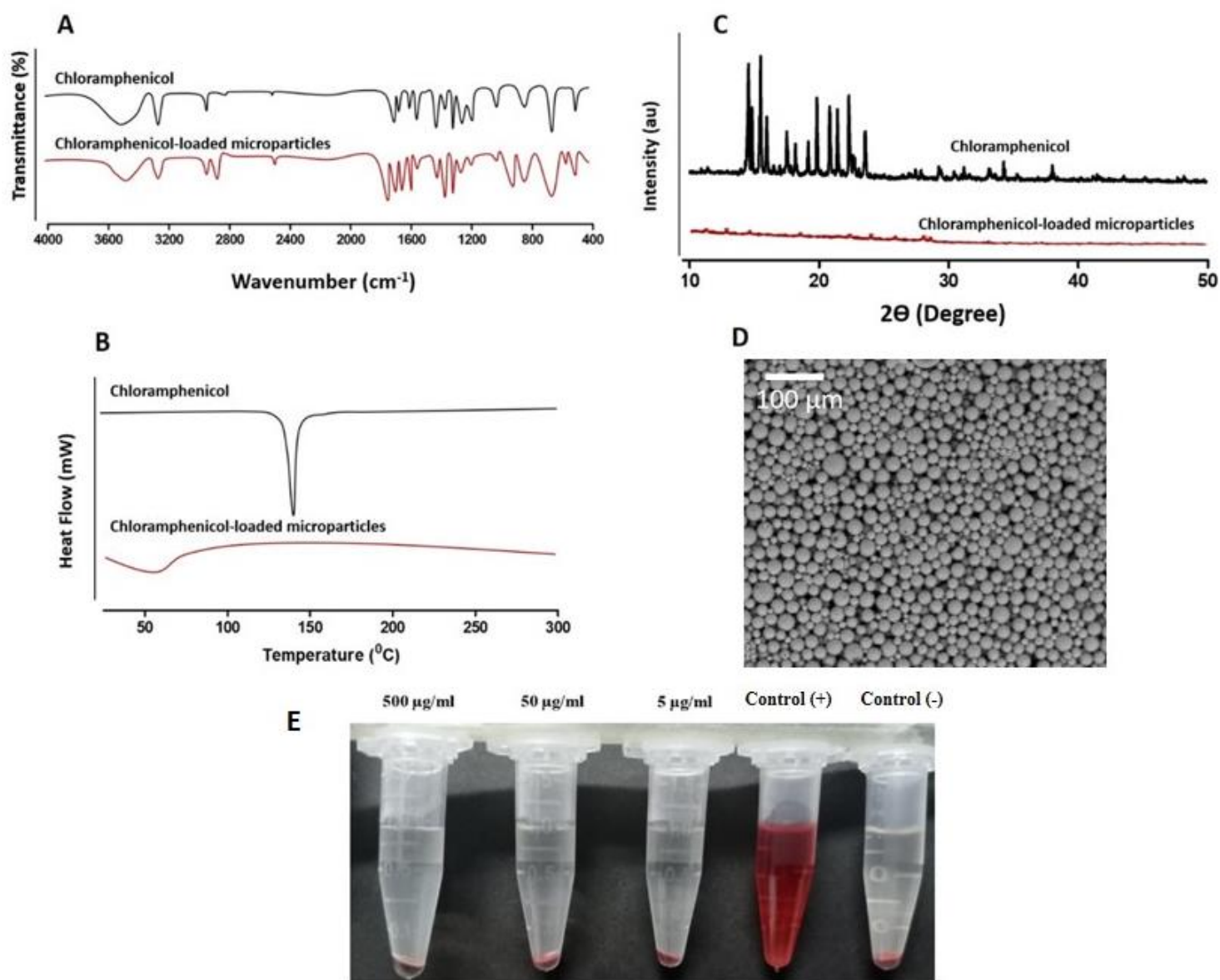
	Y1	Y2	Y3	Y4
<b>Predicted</b>	28.59	0.011	42.61	21.53
<b>Observed</b>	24.33	0,010	40,96	19.12
<b>Predicted Error (%)</b>	<b>14.89</b>	<b>8,727</b>	<b>3,87</b>	<b>11.19</b>

551 It was found zeta potential measurements for microparticles (MPs) was  $-7.54 \pm 0.65$  mV.  
 552 The presence of the ionized carboxylic groups of PCL was the cause of the negative zeta potentials  
 553 observed for MPs <sup>42</sup>. The amount of MPs adhering to the bacterial cell surface of SA corresponds  
 554 closely with the values of zeta potential difference <sup>43</sup>. It has been previously reported that the zeta  
 555 potential value of SA was -35.6 mV.<sup>44</sup> As a result, it is possible to infer that the higher of zeta  
 556 potential difference between SA and MPs as a straightforward and brief description of the good  
 557 adsorption mechanism in bacteria-MPs systems.

558 To confirm that there had been no chemical interactions between CHL and the ingredients  
559 used to create MPs, FTIR analysis was employed. Chloramphenicol's characteristic infrared peaks  
560 show the existence of a free hydroxyl group, N-H stretching, aromatic stretching, CH<sub>2</sub> asymmetric  
561 and symmetric stretching, and C-O stretching.<sup>11</sup> Figure 5A displays the FTIR spectra CHL, and  
562 CHL-loaded MPs. The CHL spectrum display had absorption peaks of 3487 OH stretching  
563 vibration, 3218 NH stretching vibration, 2978 aromatic C-H stretching vibration, 1686 C=O  
564 stretching vibrations, and 1549 NO<sub>2</sub> stretching peak. These peaks are similar to those reported in  
565 previous investigations.<sup>22</sup> It has been concluded there were no chemical interactions between CHL  
566 and the components used to generate CHL-loaded MPs, and all of the characteristic CHL peaks  
567 were identical in the MPs, demonstrating the existence of all key functional groups of CHL.

568 Figure 5B displays the differential scanning calorimetry (DSC) analysis findings for CHL  
569 and CHL-loaded MPs. Because CHL crystals have melting temperatures around 148°C, the data  
570 exhibited pronounced endothermic peaks. However, with CHL-loaded MPs, this peak was not seen.  
571 Figure 5C shows the XRD diffractograms of the pure CHL and its MP formulations. Due to the  
572 strong crystalline features of CHL, sharp characteristics peaks of CHL were seen at 2θ values from  
573 15–24. The spectra obtained are the same as the results reported in previous studies.<sup>11</sup> These peaks,  
574 however, were not visible in MPs formulations, which is identical to the findings of the DSC  
575 investigation. The total encapsulation of CHL in amorphous or solution form in the MP polymers  
576 utilized in this work may be the source of the lack of the CHL peak in the DSC and XRD analyses.  
577 However, the lack of the CHL peak did not affect the pharmacological activity of CHL, which is in  
578 agreement with FTIR results that showed all of the characteristic CHL peaks were identical in the  
579 MPs, demonstrating the existence of all key functional groups of CHL.

580



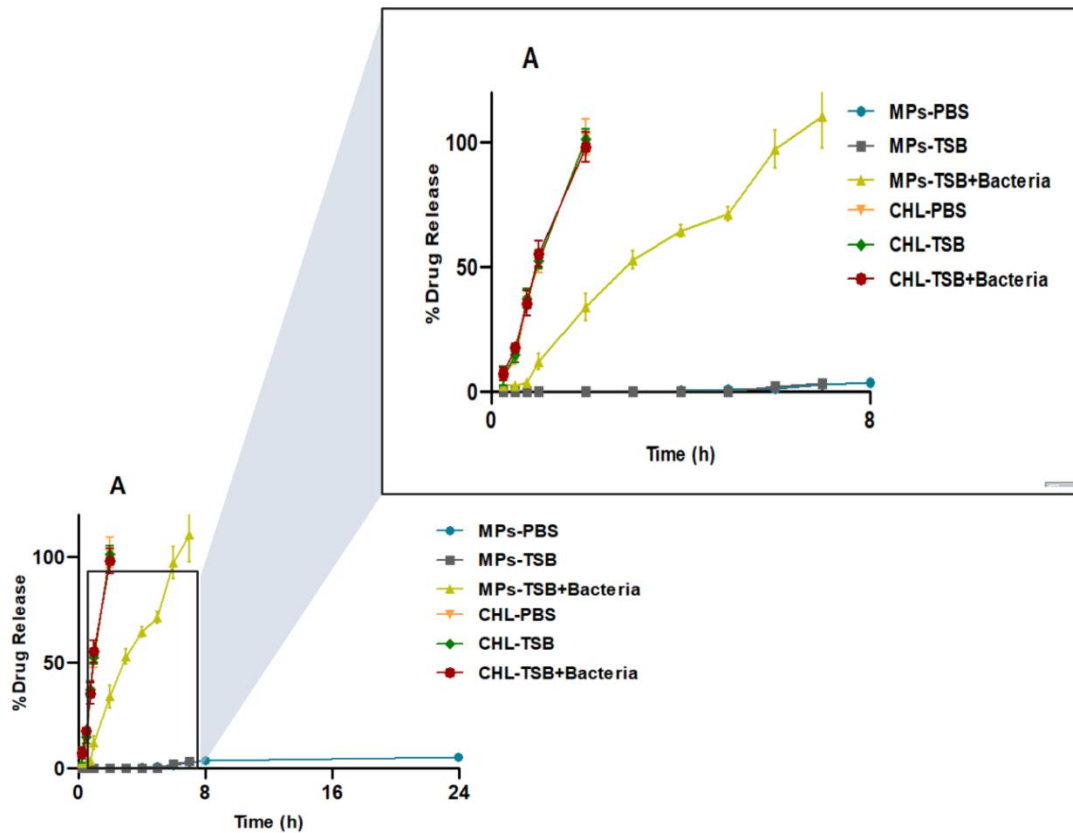
582 **Figure 5.** FTIR spectra of CHL and CHL-loaded MPs (A). DSC thermogram of CHL and CHL-  
 583 loaded MPs (B). X-ray diffractogram of CHL and CHL-loaded MPs (C). SEM images of CHL-  
 584 loaded MPs (The white scale bar represents a length of 100  $\mu\text{m}$  in each case) (D), Determination of  
 585 hemolytic activity of CHL-loaded MPs at concentration ranges of 5  $\mu\text{g/mL}$ , 50  $\mu\text{g/mL}$ , 500  $\mu\text{g/mL}$   
 586 by comparing the color of the serum and plasma with that of positive and negative controls (E).

587           **3.5. Hemolytic activity of CHL-loaded MPs.** Hemolytic activity study in mammalian  
588 erythrocytes is used to assess antimicrobials' bacterial selectivity of toxicity. According to our  
589 investigation, the hemolysis value for MPs was 0% through measurements using the  
590 spectrophotometric method. It has also seen by clearer and more translucent erythrocyte cells that  
591 have been measured after MP therapy and compared to the positive control (distilled water) (see  
592 Figure 5E). Manufacturing CHL-loaded MPs did not exhibit significant hemolysis (5%) in any of  
593 the tested doses (5, 50, and 500 ppm). The results showed that MP compositions are safe to use  
594 since hemolysis indices lower than 5% are considered safe.<sup>45</sup>

595           **3.6. In-vitro release kinetic study of CHL-loaded MPs.** Studies on kinetical drug release  
596 provide the information of how long a drug substance stays in the system. The kinetical release  
597 study of CHL and CHL-loaded MPs was conducted in both the absence and presence of the bacteria  
598 in several media (See Figure 6). We chose PBS as the initial kinetics media for investigation because  
599 it reflects typical skin fluid media. Regarding in CHL-loaded MPs, the findings revealed in PBS  
600 media that  $5.13 \pm 0.72\%$ , was the percent CHL determined after 24 hours in its media. To evaluate  
601 drug release patterns and show that the release profile was solely controlled by bacteria, we also  
602 looked at fluid imitating illness (TSB) without bacteria. The findings revealed the percentage of  
603 CHL released in TSB media was  $5.34 \pm 1.06$  after 24 hours. It was discovered that both media had  
604 lower CHL levels compared to pure chloramphenicol. This was because there was no bacterial  
605 enzyme stimulus to lyse the polycaprolactone polymer, which would have allowed the medication  
606 to stay stable in the microparticle polymer matrix. According to the statistical analysis, there was  
607 no statistically significant difference between the release profiles of CHL-loaded MPs and  
608 chloramphenicol when compared to PBS and TSB media ( $p > 0.05$ ). This demonstrated that release

609 in the bacterial responsive microparticle system was unaffected by the environment devoid of  
610 bacteria.

611 Regarding the *in vitro* release profile of CHL-loaded MPs on TSB medium with presence  
612 of bacteria, the percentage of CHL determined after 24 hours in CHL-loaded MPs was  $110.66 \pm$   
613  $13.04\%$ . The TSB Media that presence of bacteria demonstrated higher drug release. This is due to  
614 bacteria culture in media producing lipase enzymes that were used to lyse the MPs matrix and detect  
615 chloramphenicol concentrations in the medium.<sup>46</sup>



616

617 **Figure 6.** *In vitro* release profile of CHL-loaded MPs and CHL in several media

618

(mean  $\pm$  SD, n= 3)

619

620 The statistical analysis revealed that the bacterial TSB media with PBS and the absence of  
621 bacteria had noticeably different release profiles. Figure 6 shows the levels of pure CHL in all test  
622 medium reached close to 100% after 3 hours of administration. The MPs preparation in media that  
623 contained bacteria reached up to 100% after 8 hours. It is suggested that microparticle production  
624 can sustain the release of CHL, hence extending the period of exposure to bacteria. This is a good  
625 strategy for the administration of antibiotics.

626 The increased release of CHL from MPs in the presence of bacteria is due to the fact that  
627 the presence of bacteria can produce enzymes specifically to accelerate degraded PCL matrix. This  
628 is supported by the fact that no drug release was observed when the MPs were suspended in the  
629 sterile culture media. This outcome aligned with that of Wu et al., who found that the inclusion of  
630 an enzyme stimulate PCL degradation by a factor of 1000 fold in comparison to degradation in an  
631 aqueous medium alone.<sup>47</sup> The suggested technique has the potential for selective delivery at  
632 infection sites, as seen by the significant difference in CHL release depending on the presence and  
633 absence of the bacterium. These findings therefore show that loading CHL into a flexible MPs  
634 system can prevent release at nonspecific locations.

635 To explain the CHL release profile of CHL-loaded MPs, the results from the *in vitro* release  
636 investigations on bacterial growth medium were subsequently fitted to five mathematical models.  
637 Table 4 displays the findings of the CHL-laoded MPs and CHL release kinetics investigation.

638

639

640

641

642

**Table 4.** Representative Kinetic model of drug release MP-CHL

Formulation	Kinetic Model				
	Zero Order	First Order	Higuchi	Korsmeyer-Peppas	Hixson-Crowell
CHL	0.9851	0.8334	0.8167	0.9391	0.9226
CHL-loaded MPs	0.9902	0.6800	0.7658	0.9132	0.7716

644 According to *in vitro* release tests, CHL-loaded MPs and pure chloramphenicol matched the  
645 kinetic models proposed by zero order (ZO). The prospective use of ZO drug delivery systems may  
646 make it possible to accurately control release kinetics and extend therapeutic drug concentration  
647 windows. As a result, these systems can increase therapeutic effectiveness, reduce adverse effects,  
648 and decrease administration frequency, all of which can lead to improved patient compliance and  
649 disease management.<sup>48</sup> This approach has been chosen to characterize drug removal from the  
650 polymeric model dependent on polymer response with stimulus bacteria and dispersion of MPs  
651 drugs.

### 652 3.7. In-vitro antibacterial assays

653 **3.7.1. MIC and MBC.** Furthermore, investigation was conducted into the antibacterial  
654 activity of formulations containing free CHL and CHL-loaded MPs. Table 5 describes the  
655 comparisons of MIC and MBC values between the CHL solution and their MP formulations. The  
656 MIC value for CHL-loaded MPs against SA ATCC 25923 was 12.5 µg/mL, which same that of free  
657 CHL (12.5 µg/mL); see table 4. The MBC value of CHL-loaded MPs (25 µg/mL) was equal to the  
658 MBC of free CHL (25 µg/mL).

659 Based on the findings, CHL and CHL-loaded MPs may be classified as an intermediate  
 660 category for the inhibition of SA strains. According to the clinical and laboratory standards institute  
 661 criteria for MIC  $\leq 8$   $\mu\text{g/mL}$  was considered susceptible,  $\leq 16$   $\mu\text{g/mL}$  was considered intermediate,  
 662 and  $\geq 32$   $\mu\text{g/mL}$  was considered resistant.<sup>49</sup>

663 **Table 5.** MIC of free CHL and CHL-loaded MPs

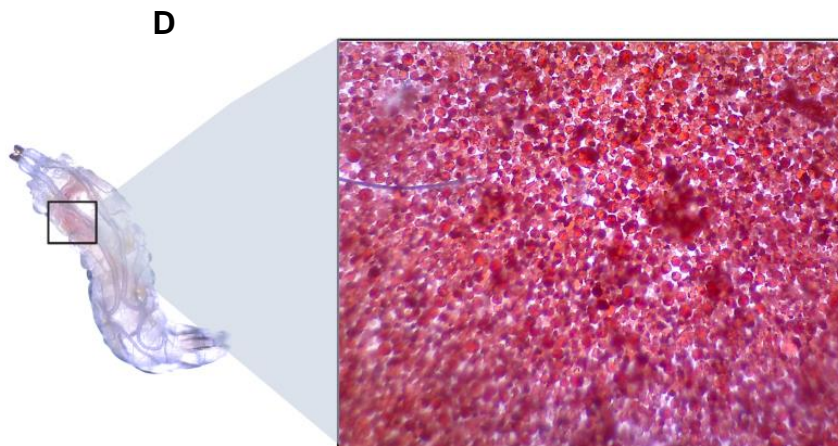
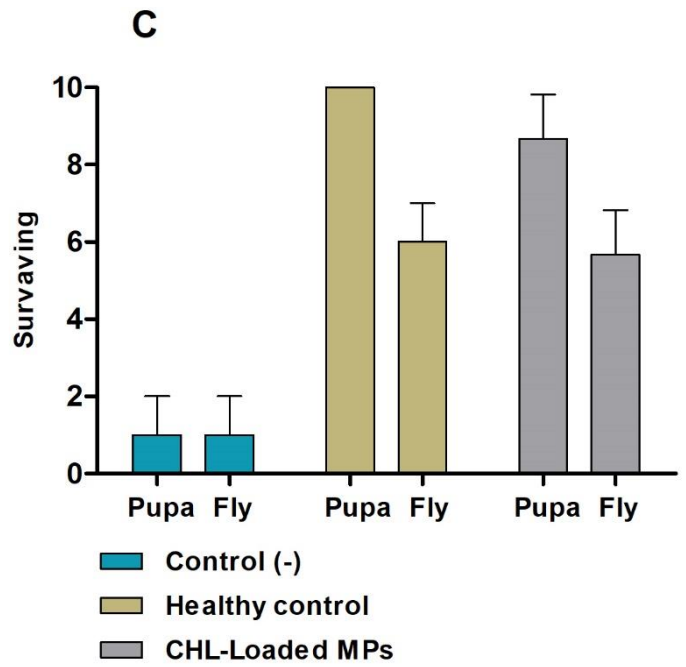
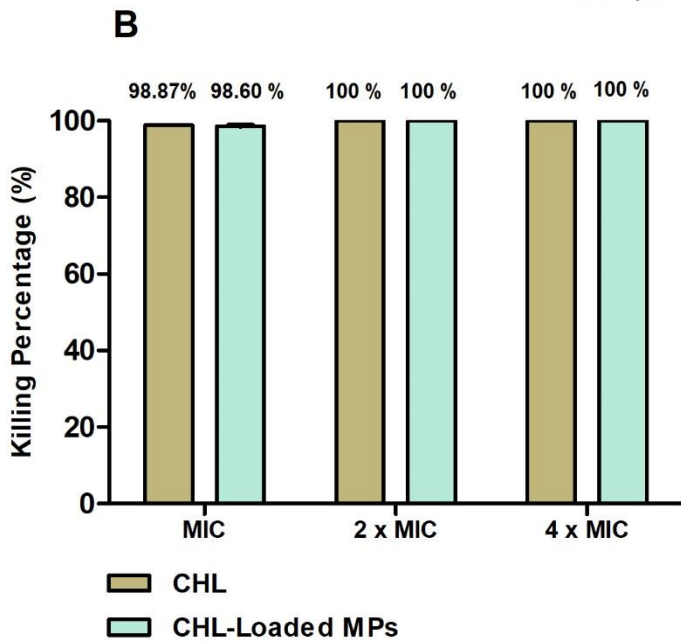
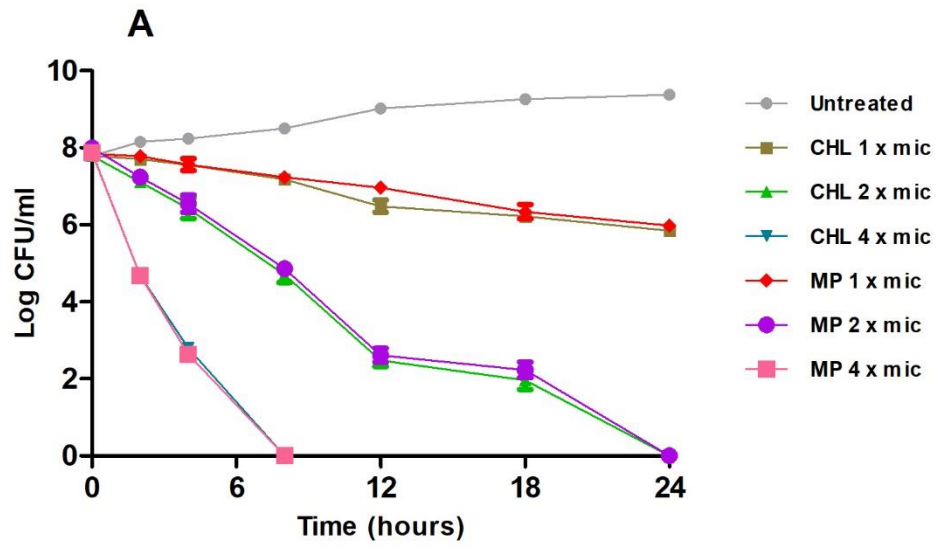
<b>Antimicrobial properties</b>	<b>Concentration (ppm)</b>						
	200	100	50	25	12.5	6.25	3.125
CHL	(-)	(-)	(-)	(-)	(-)	(+)	(+)
CHL-Loaded MPs	(-)	(-)	(-)	(-)	(-)	(+)	(+)

664 All MBC values in this investigation were greater than MIC values, demonstrating that  
 665 higher CHL concentrations were necessary to inhibit the bacterial cultures. When comparing the  
 666 ratio of MBC to MIC, it was discovered that this ratio was always 4. Bacteriostatic is indicated by  
 667 a ratio of less than 4 and bactericidal by a ratio of 4.<sup>50</sup> As a result, our research suggested that CHL  
 668 and CHL-loaded MPs both have bactericidal properties.

669

670

671



673 **Figure 7.** (A) Time kill assay of CHL and CHL-loaded MPs against SA (means  $\pm$  SD, n=3). (B)  
674 Anti-infection activity in 96 well microtiter plate of CHL and CHL-loaded MPs against SA (means  
675  $\pm$  SD, n=3). (C) Survival of in psh[1];;modSP[KO] drosophila melanogaster larvae upon 30 minutes  
676 of oral infection with SA in terms of pupae and adult flies' parameter. (D) Trial study to observation  
677 in coloring microparticles after concomitant oral administration in drosophila larva model.

678 **3.8. In vivo investigation on a Drosophila larval infection model.** The evaluation of  
679 antimicrobial activity of CHL-loaded MPs against SA ATCC 25923 was carried out using  
680 Drosophila larvae as the infection model. Drosophila larval has recently been used in the infection  
681 experiment to demonstrate the virulence of three clinical strains of SA.<sup>30</sup> From previous research,  
682 it is evident that the larval model of infection is easy-to-use and can serve as a suitable host for SA  
683 infection, thus beneficial to be used as a rapid in vivo screening platform. In our investigation, we  
684 employed the immunodeficient psh[1];;modSP[KO] line. Psh and ModSP, a mutant line lacking  
685 two important components in the Toll pathway. The absence of these components thus prevent the  
686 production of AMPs, which is necessary for the activation of humoral innate immunity in response  
687 to SA infection in Drosophila.<sup>51,52</sup> This results in a condition that resembles immunodeficiency,  
688 facilitating the easy preparation of an infection model. Such mutant flies have been demonstrated  
689 to succumb to pathogens faster than their wild-type counterparts.<sup>53,54</sup> Through this model of  
690 infection, we can rule out the role of toll-mediated innate immunity responses in Drosophila that  
691 play a major role in SA infection thereby confirming the antibacterial effect of the drug candidates.

692 For the preliminary investigation, we tested dyed microparticles to examine if the  
693 microparticles created could be delivered orally to a Drosophila larval model (see Figure 7D). If the  
694 MPs entered orally, they were visible on the larvae abdomen. Based on the findings, the MPs were  
695 successfully visible on the larva abdomen under a microscope after concomitant oral administration.

696 Infection parameters were assessed by counting the number of pupae that have successfully  
697 formed, and how many pupae succeeded in becoming adult flies. If the infected larva grow to form  
698 pupae, there are two chances that a pupa will not develop into an adult fly, according to our  
699 hypothesis. The first possibility is that an increase bacterial infection burden causes larvae to die  
700 during the pupa stage. Another possibility is that the infection causes the energy generated to focus  
701 on infection recovery, leaving insufficient energy for the pupa to become an adult fly. Based on  
702 Figure 7C, infected larvae without treatment showed larval death; only a few survived to become  
703 pupae and adult flies. According to several studies, the increased mortality rate of the dying host  
704 has been connected to bacterial load.<sup>52</sup> Since giving CHL-loaded MPs, which was mixed on fly  
705 food, increased the survival rate of infected *Drosophila* larva. Because this finding is not  
706 significantly different than in healthy controls ( $p > 0.05$ ), it is tempting to assume that this phenotype  
707 was caused by the prevention of bacterial growth *in vivo* model. According to these results, there  
708 are two possible steps of MPs system that could accelerate the killing of bacteria, thereby preventing  
709 larvae death. The MPs were initially made linked to the infection by the outer layer of PCL. After  
710 that, the presence of the bacterial strains lipase destroyed PCL layers, causing the release of CHL  
711 from MPs, which then killed the bacteria. This supports earlier researchers' findings that toll  
712 immunodeficient flies were more susceptible to bacterial infection. Additionally, similar outcomes  
713 were seen in *psh[1];modSP[KO]* mutant flies that lacked cellular innate immunity and have a lower  
714 survival rate than healthy controls.<sup>52</sup> This mutant fly might survive longer in the presence of CHL-  
715 loaded MPs because it lacks the cellular innate immunity that is known to defend against SA. These  
716 findings revealed that the antibacterial activity of CHL-loaded MPs against SA was not based on  
717 activation of cellular immunological responses, but rather by direct interactions between chemicals  
718 present in the MPs and bacteria.

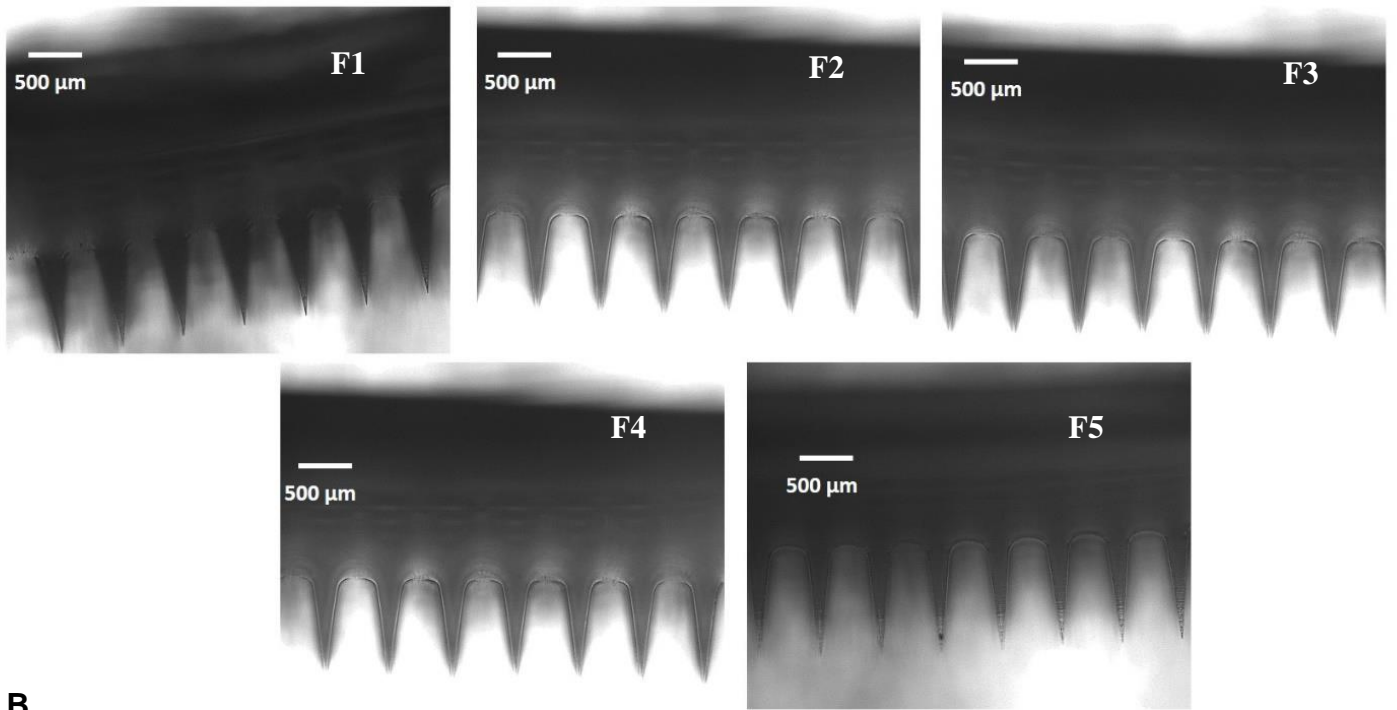
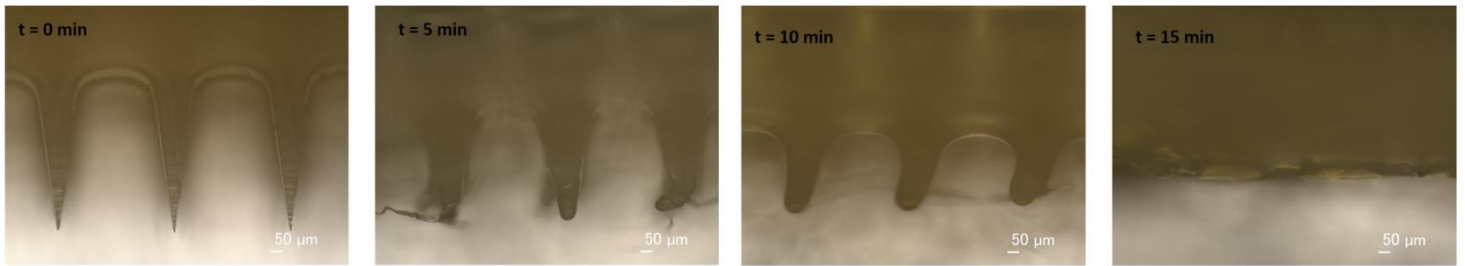
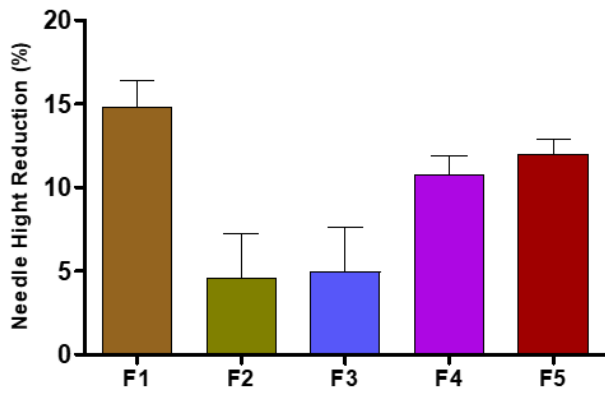
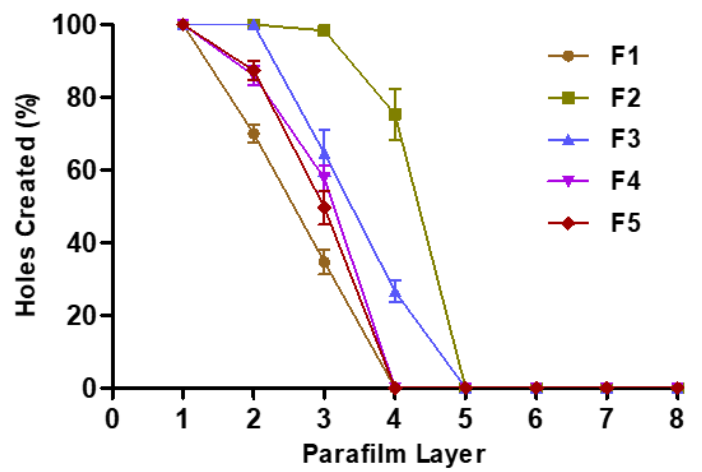
719           **3.9. Fabrication of two-layered MNs.** CHL is ineffective for the topical treatment of skin  
720 infections due to its hydrophobic chemical components, which limits effective cutaneous  
721 penetration. Barriers to effective penetration include thicker skin and the formation of biofilms that  
722 inhibit drug penetration to the site of infection. Therefore, the CHL-loaded MPs in this investigation  
723 were further formed into MNs arrays to enhance the penetration of the antibacterial agents and can  
724 be disrupted responsively with contact the infection site of bacteria. The dissolving MNs were created  
725 by combining PVA and PVP, two water soluble polymers. In our earlier research, dissolving MNs  
726 with adequate mechanical characteristics could not be created using a single polymer.<sup>23,25</sup> In  
727 contrast, the C=O groups of PVP and the -OH groups of PVA interact to create a hydrogen bond,  
728 increasing the mechanical strength of MNs.<sup>25</sup> Figure 8A illustrates the morphologies of MNs seen  
729 under a light microscope, demonstrating that all DMN formulations created sharp needles. In this  
730 investigation, two-layered MNs formulations with various polymer concentrations were created to  
731 find the best mechanical properties.

732           **3.10. Evaluation of mechanical and insertion properties of dissolving MNs.** The  
733 mechanical toughness of the MNs arrays was assessed to ensure that MNs arrays were strong  
734 enough to resist compression. The ability of MNs to be inserted into the skin is important since the  
735 needle must be able to break through the stratum corneum in order to deliver the substance drug  
736 into the normal skin layers.<sup>55</sup> The proportion of MNs, the needles height that was reduced in this  
737 study following 32 N/MN array that is equivalent to human hand compression pressure. A  
738 calculation was made to determine mechanical strength. The mechanical characteristics of each  
739 formulation are shown in Figure 8C as a percentage reduction in MNs, which compared height of  
740 needle before application pressure force. For MNs-F1, MNs-F2, MNs-F3, MNs-F4, and MNs-F5,  
741 the decreases in MN height were determined to be  $14.82 \pm 1.55\%$ ,  $4.56 \pm 2.66\%$ ,  $4.96 \pm 2.66\%$ ,

742 10.73 ± 1.17%, 11.97 ± 0.89%, respectively. As a result, the mechanical characteristics of the  
743 dissolving MNs arrays were unaffected by the formulation of CHL-loaded MPs. Despite the fact  
744 that F4 and F5 had larger percentages of height losses than F2 and F3, several studies have indicated  
745 that DMN formulations with a percentage of height decrease of about 25% were acceptable.<sup>56</sup>

746 As a skin stimulant for the insertion qualities force, eight layers of Parafilm<sup>®</sup> were used.  
747 This model has been certified to mimic human skin for MNs insertion investigations<sup>55</sup>. The study's  
748 results are shown in Figure 8D. The formulation of the MN regarding different polymer  
749 concentrations (PVA and PVP) as mentioned previously, had no effect on any of the MNs' insertion  
750 qualities ( $p > 0.05$ ), similar to how it had no effect on the mechanical properties. Four layers of  
751 Parafilm<sup>®</sup> were able to be penetrated by the MN arrays. The typical thickness of each layer of  
752 Parafilm<sup>®</sup> is 126 μm. Thus, DMNs were placed up to a height of 378 μm. F1, F4, and F5 produced  
753 holes in the third layer that were responsible for 34.66 ± 5.85%, 57.66 ± 6.11%, and 49.66 ± 8.02%,  
754 respectively, of the total holes. F2 and F3 produced holes in four layers and were respectively  
755 responsible for 75.33 ± 12.01% and 26.66 ± 5.13%, of the total holes. As a result, F2 was chosen  
756 for further testing since it had a good penetration layer and holes created compared to other  
757 formulas.

758 To estimate how long it would take for the needles to dissolve in the skin after  
759 administration, dissolution experiments of MN formulations incorporating drug-loaded MPs were  
760 examined. According to Figure 8B, breakdown of MNs while in the skin occurred after 15 minutes,  
761 with needle disintegration and a drop in height being apparent after 5 minutes. This showed that the  
762 formulation met acceptable criteria for MNs formulations.

**A****B****C****D**

765 **Figure 8.** (A) Images taken under a light microscope of the MP-containing MN formulations. (B)  
766 Morphology of dissolving microneedle containing CHL-Loaded MPs after skin administration. (C)  
767 The percentage height reduction of needles on the arrays formulated containing free CHL and CHL-  
768 loaded MPs compared to blank MN arrays (means  $\pm$  SD, n=3). (D) Percentage of holes created in  
769 Parafilm<sup>®</sup> layers, using an insertion force of 32N/array for MN formulations containing CHL-  
770 loaded MPs (means  $\pm$  SD, n=3).

771 **3.11. Calculation of drug content localized to the needles.** Upon drying the MN arrays, it  
772 was found that each one contained 70.58  $\mu$ g CHL, with a percent recovery of  $98.09 \pm 1.82\%$ . The  
773 dose of CHL in one MN array in the succeeding trials was thus reflected by these medication  
774 quantities.

775 **3.12. Stability Test of MPs-CHL loaded into Dissolving Microneedle.** The capacity of the  
776 formulations to preserve the MPs stability, especially their sizes, PDIs, entrapment efficiency, drug  
777 loading and zeta potentials, is one of the essential criteria in the formulation of MPs into dissolving  
778 MNs. Table 6 shows the MPs characteristics in the MNs formulations. These results imply that the  
779 particle size, EE%, DL%, and zeta potential of CHL-loaded MPs were not significantly ( $p > 0.05$ )  
780 affected by the inclusion of MPs into MNs arrays. Regarding the PDI value, it increased after being  
781 added to MNs but still produced a PDIs below 0.05, indicating that the formulations are still  
782 homogeneous and monodisperse.

783

784

785

786

787

788 **Table 6.** Particle size, PDI, zeta potential, EE, and DL of formulations of CHL-loaded  
 789 MPs in MNs formulation (means  $\pm$  SD, n = 3).

<b>Characteristics</b>	<b>Days 0</b>	<b>Days 3</b>	<b>Days 7</b>	<b>Days 10</b>
<b>Particle Size (<math>\mu\text{m}</math>)</b>	25.43 $\pm$ 1.32	24.65 $\pm$ 1.54	25.65 $\pm$ 1.31	25.87 $\pm$ 1.45
<b>PDI</b>	0.054 $\pm$ 0.003	0.043 $\pm$ 0.004	0.051 $\pm$ 0.005	0.049 $\pm$ 0.004
<b>Zeta Potential (mV)</b>	-7.19 $\pm$ 0.44	-7.09 $\pm$ 0.36	-7.11 $\pm$ 0.52	-7.05 $\pm$ 0.43
<b>EE (%)</b>	39.69 $\pm$ 2.76	39.54 $\pm$ 2.65	38.56 $\pm$ 3.01	38.44 $\pm$ 2.41
<b>DL (%)</b>	18.43 $\pm$ 1.34	18.31 $\pm$ 1.17	18.16 $\pm$ 1.37	18.14 $\pm$ 1.29

790  
 791 **3.12. Ex vivo dermatokinetic studies.** The main goal in this investigation was to determine  
 792 of dermatokinetic profile of CHL- loaded MPs in skin layers, where SA colonizes, infects, and  
 793 produces wound skin infection. In order to do this, a dermatokinetic analysis was created and carried  
 794 out to examine the CHL release kinetics from MPs following MNs application. This study employed  
 795 normal skin and infected model on rat skin tissue to prove that the presence of a bacterial infection  
 796 is only impact on the release of chloramphenicol in the skin, chloramphenicol secreted by MPs was  
 797 assessed. This was done in order to determine how much CHL was retained in the skin by vortexing  
 798 the skin samples with water at each interval. Our findings demonstrated that this method would only  
 799 extract CHL produced by MPs because no CHL was discovered in the MP dispersion's supernatant  
 800 after sample vortexing.

801 The dermatokinetic profile of our method in this investigation was compared of MNs  
 802 containing CHL-loaded MPs (MNs-CHL MPs) and without MPs formulation (MNs-CHL). To  
 803 compare their effectiveness with the previously stated methods, the dermatokinetic properties of a  
 804 conventional cream containing CHL (cream-CHL) and cream containing CHL-loaded MPs (cream-

805 CHL MPs) were also evaluated. Figure 9a–b shows the concentration of CHL released with another  
806 approach delivery system in the skin vs. application time following its application. The  
807 dermatokinetic parameters of CHLs, including  $C_{max}$ ,  $T_{max}$ ,  $T_{1/2}$ , AUC, and MRT, also were  
808 calculated as shown in Table 6. This result demonstrated, in the absence of bacterial growth in  
809 normal skin, MNs-CHL MPs produced CHL concentrations significantly lower than MNs-CHL  
810 ( $p < 0.05$ ). This phenomenon also occurs in the application system for conventional cream  
811 preparations. Due to the justifications given for the  $C_{max}$  results, the  $T_{max}$  values of CHL from  
812 MNs-CHL MPs was also discovered to be significantly lower ( $p < 0.05$ ) than those from the other  
813 formulations in normal skin. This suggested that the nonspecific release (normal skin test) of CHL  
814 may be prevented by incorporating CHL into MPs. The level of  $C_{max}$  of CHL in conventional  
815 cream preparations was significantly lower than in MNs preparations ( $p < 0.05$ ). This was due to  
816 the hydrophobic chemical components of CHL and CHL-loaded MPs, which limit effective  
817 cutaneous penetration. This is a proof concept that the application of the MNs system can increase  
818 the concentration drug penetration for dermal drug administration.

819       Regarding *ex vivo* infection models using SA, the release of chloramphenicol from MNs-  
820 MPs was significantly enhanced ( $p < 0.05$ ) compared to MNs-CHL. According to the findings of  
821 this study, CHL encapsulation in PCL matrix, may boost CHL concentration through two separate  
822 methods. The MPs' initial adhesion to the colony infection was made easier by the PCL outer layer.  
823 After then, the environment was exposed to bacterial strains whose lipase broke down PCL layers,  
824 releasing CHL from MPs.

825       Regarding AUC, it was discovered that the AUC values of CHL from MNs-MPs in *ex vivo*  
826 infection models were considerably greater ( $p > 0.05$ ) than those of other formulations,  
827 demonstrating the improved *ex vivo* skin bioavailability of our strategy. To assess retention duration

828 in the skin, we examined the MRT parameter, which shows how long drug molecules stay in skin  
829 tissue. It was discovered that the MRT values of CHL from DMN-MPs were significantly higher  
830 ( $p < 0.05$ ) than those of MNs-CHL, cream-MPs, and cream-CHL, demonstrating a longer retention  
831 period in the skin. Because of the enhanced MRT, a shorter application period for CHL in the  
832 treatment of skin infections may be feasible. As a result, it could influence patients to adopt this  
833 approach. Our results suggest that chloramphenicol may be effectively transferred into an *ex vivo*  
834 infection model via a combination of responsive MPs and MNs.

835 **3.13. Anti-infection activity in *ex vivo* model of infection on rat skin.** The reduction of  
836 bacterial bioburdens in *ex vivo* infection models made of SA was examined by measuring the viable  
837 cell counts to evaluate the effectiveness of this strategy. In an *ex vivo* rat skin wound model, post-  
838 infection CFU counts revealed a significant decrease in microbial load in all various treated wounds  
839 compared to untreated wounds. Figure 10A–B displays the study's findings. Regarding cream  
840 conventional preparations, with only around  $90.77 \pm 6.46\%$  of the bacterial bioburden reduced after  
841 24 hours. While, on MPs-CHL were made into cream conventionally resulting in  $58.88 \pm 8.38\%$   
842 decrease in bacterial bioburden, resulted in the lowest anti-infection performance in *ex vivo*  
843 infection models

844 Regarding DMNs preparation, CHLs were applied to both bacterial *ex vivo* infection models,  
845 and the results showed  $96.38 \pm 1.27\%$  decrease in bacterial bioburden after 24 hours of treatment.  
846 In DMNs containing MPs-CHL showed  $99.99 \pm 0.01\%$ . Although the  $C_{max}$  of MN-free CHL was  
847 greater than the MBC of CHL to bacterial strain, the retention period of CHL after application was  
848 less than the time required by CHL to totally kill the bacterial. Consequently, only around  $96.38\%$   
849 of the bacterial loads of strain decreased after the administration of MN-free CHL. This suggested  
850 that DMNs could enhance the effectiveness of CHL as anti-infection agents. A number of studies

851 have demonstrated that adding antibacterial drugs to MNs increased their antibacterial activity.  
852 <sup>57,20,33,58</sup> Essentially, the adoption of this strategy was able to completely remove the SA since DMN-  
853 MPs had the optimum *ex vivo* skin bioavailability in the dermatokinetic testing. Consequently, there  
854 were two key advantages of administering CHL that were loaded with PCL-MPs and delivered *via*  
855 DMNs.

856 The dermatokinetic profiles in this investigation show that manufacturing CHL into MPs  
857 could be improved and controlled using this method as opposed to conventional cream formulation.  
858 This method may increase the effectiveness of CHL in *ex vivo* infection models in rat skin generated  
859 by SA.

860 **Table 6.** Lists the dermatokinetic characteristics of chloramphenicol in uninfected rat skin as well as ex infection models  
 861 created by SA after the administration of DMN-MPs, DMN-CHL, cream-MPs and cream-CHL. (means SD, n=3)

<b>Condition</b>	<b>Formulation</b>	<b>Cmax</b> ( $\mu\text{g}/\text{cm}^3$ )	<b>Tmax (h)</b>	<b>T1/2 (h)</b>	<b>AUC 0-t</b> ( $\mu\text{g}/\text{cm}^3\cdot\text{h}$ )	<b>AUC 0-inf_obs</b> ( $\mu\text{g}/\text{cm}^3\cdot\text{h}$ )	<b>MRT (h)</b>
<b>Normal Skin</b>	DMN-MPs	0.58 ± 0.11	6.33 ± 1.15	12.30 ± 8.87	6.33 ± 1.20	10.09 ± 5.40	21.06 ± 14.16
	DMN-CHL	36.27 ± 1.01	2.00 ± 0.00	4.89 ± 1.35	97.81 ± 2.62	99.41 ± 3.44	3.87 ± 0.76
	Cream-MPs	0.12 ± 0.07	24.00 ± 0.00	N/A	1.41 ± 0.83	N/A	N/A
	Cream-CHL	2.08 ± 0.47	5.00 ± 0.00	7.02 ± 2.14	7.99 ± 1.50	9.59 ± 1.62	13.06 ± 4.91
<b>Infected Skin</b>	DMN-MPs	35.73 ± 1.43	6.00 ± 0.00	19.79 ± 6.03	375.38 ± 9.57	737.55 ± 160.00	31.67 ± 8.62
	DMN-CHL	35.86 ± 1.63	2.00 ± 0.00	5.76 ± 3.46	92.95 ± 1.93	94.06 ± 2.48	3.48 ± 0.33
	<b>By SA</b> Cream-MPs	2.67 ± 0.29	6.00 ± 0.00	6.39 ± 2.05	9.58 ± 1.24	10.52 ± 1.77	9.81 ± 1.94
	Cream-CHL	2.19 ± 0.46	5.00 ± 0.00	6.39 ± 2.67	8.68 ± 2.98	9.64 ± 3.43	10.03 ± 2.44

862  
 863  
 864  
 865  
 866  
 867

868

869

870

871

872

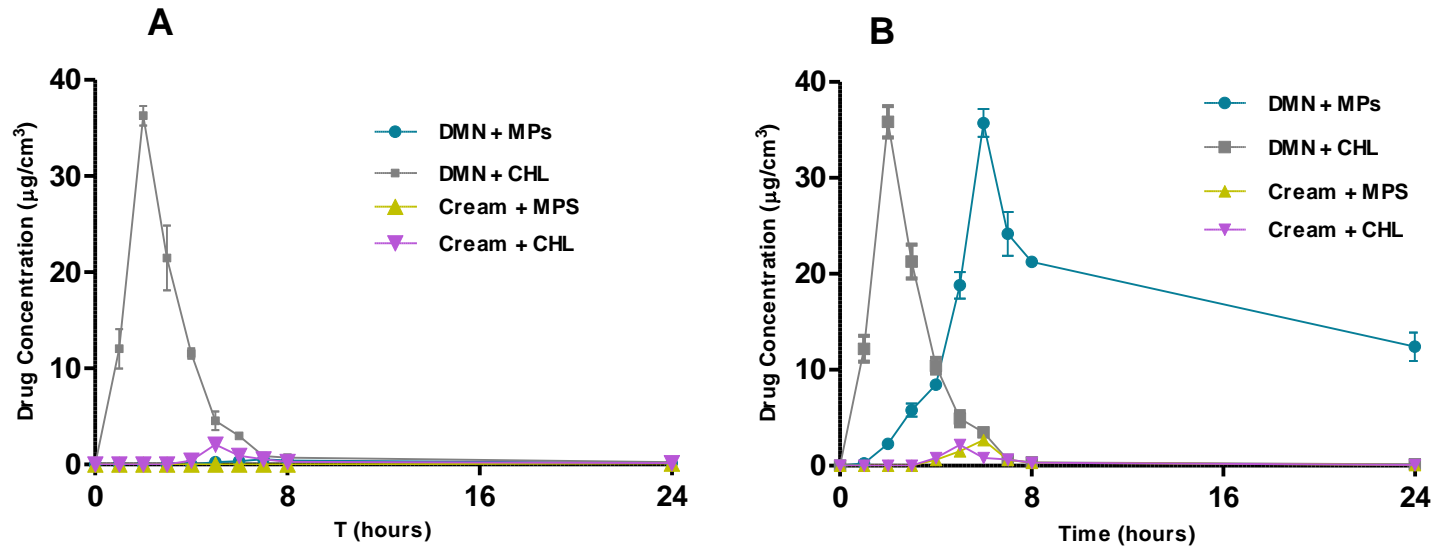
873

874

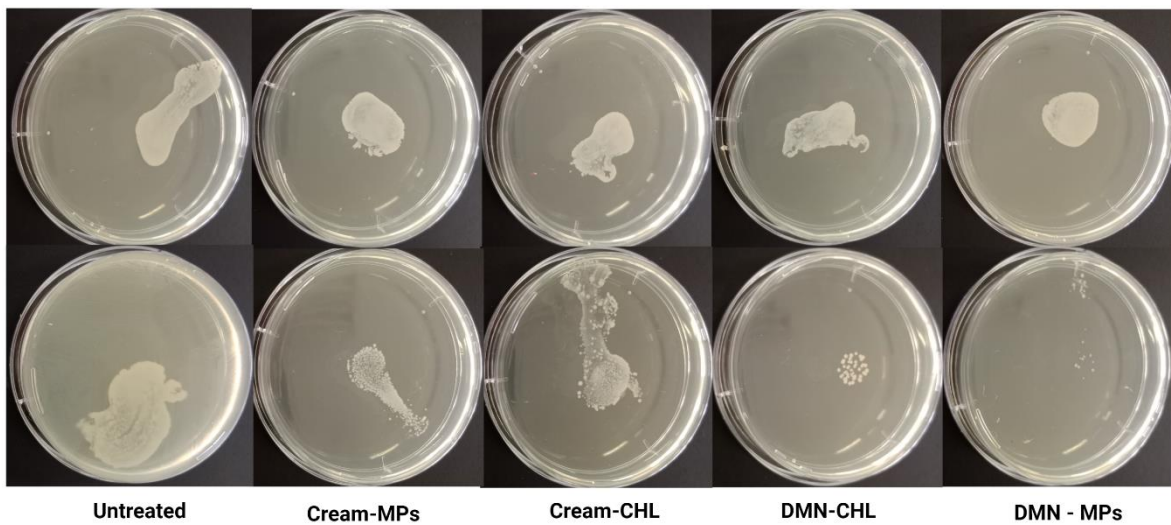
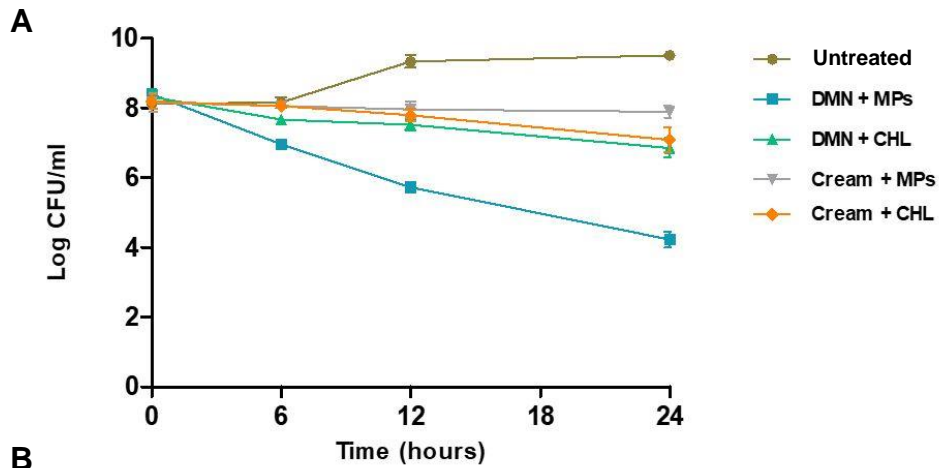
875

876

877



878 **Figure 9.** The *ex vivo* concentrations and time profiles of CHL following the application of DMN-MPs, DMN-CHL, cream-MPs and  
879 cream-CHL in non-infected rat skin (a), as well as *ex vivo* infection models formed by SA (means  $\pm$  SD, n=3) (b)



880

Untreated

Cream-MPs

Cream-CHL

DMN-CHL

DMN - MPs

881 **Figure 10.** (A) Bacterial viability (log CFU/mL) on in *ex vivo* infection models formed by SA  
 882 following the application of dissolving MNs-CHL, MNs- MPs, cream-CHL, and cream-MPs.  
 883 (means  $\pm$  SD, n=3). (B) Images of culture plates showing the *ex vivo* removal of SA infection  
 884 from wounds on rat skin at interval time 0' (above) and 24 hour (below).

885 The study's hypothesis that responsive MPs containing CHL may be successfully  
 886 delivered into the skin *via* dissolving MNs and can then demonstrate their antibacterial action  
 887 at the site of infection has been supported by the study's encouraging preliminary findings. The  
 888 ability for site-selective delivery and long retention time in the area of infection in the skin,  
 889 which may potentially increase the efficacy of antibacterial therapy for burns and chronic  
 890 wounds, are the key advantages of the selective delivery system we have developed here  
 891 compared to conventional cream dosage form. DMNs might therefore be employed to deliver

892 antimicrobial drugs topically to wounds, and their combination with certain MPs could be a  
893 feasible substitute for existing antimicrobial treatment strategies.

#### 894 **4. Conclusion**

895 To improve the antibacterial capability of CHL, specifically for the treatment of  
896 cellulitis, this study explored the novel combination strategy of bacterially sensitive MPs with  
897 dissolving MN arrays. The MPs had a diameter of about 24.33  $\mu\text{m}$  and were spherical in form.  
898 Additionally, the presence of bacterial cultures had a significant impact on the release of CHL  
899 from the MPs, demonstrating the effectiveness of this approach for targeted delivery. The  
900 evaluation of the antibacterial activity of MPs *in vitro* and *in vivo* on the mutant *Drosophila*  
901 larval infection model was carried out. This result demonstrates antibacterial properties of  
902 CHL; after being made into bacterial responsive microparticle system, its efficacy did not  
903 decrease. It is significant that adding these MPs to MN arrays made from PVP and PVA  
904 combined with these MPs gave rise to MNs with adequate mechanical characteristics and  
905 insertion capabilities. In infection tissue models in full-thickness rat skin, dermatokinetic  
906 experiments showed that the MNs improved the ability of MPs to penetrate bacterial when  
907 compared to a needle-free patch. Finally, the combined method of microparticle responsive  
908 bacteria with dissolving MNs demonstrated proof of principle for successful anti-infection  
909 action in *ex vivo* infection models, as evidenced by a reduction of bacterial bioburden up to  
910 99.99%. However, more thorough research is required, including toxicity tests and *in vivo*  
911 pharmacodynamic research using appropriate animal infection models. To confirm the work's  
912 full potential before integrating this delivery method into clinical practice and patient  
913 treatment, acceptance and usability studies should be carried out.

914

915

916

917 AUTHOR INFORMATION

918 Corresponding Author

919 Correspondence should be addressed to Andi Dian Permana (Faculty of Pharmacy, Hasanuddin  
920 University, Indonesia). Email: [andi.dian.permana@farmasi.unhas.ac.id](mailto:andi.dian.permana@farmasi.unhas.ac.id)

921 **Authors**

922 **Mukarram Mudjahid** - Department of Pharmaceutics, Faculty of Pharmacy, Hasanuddin  
923 University, Makassar 90245, Indonesia

924 **Firzan Nainu** - Department of Pharmacology and Toxicology, Faculty of Pharmacy,  
925 Universitas Hasanuddin, Makassar 90245, Indonesia

926 **Rifka Nurul Utami** - Department of Pharmaceutics, Faculty of Pharmacy, Hasanuddin  
927 University, Makassar 90245, Indonesia

928 **Anwar Sam** - Department of Pharmacology and Toxicology, Faculty of Pharmacy, Universitas  
929 Hasanuddin, Makassar 90245, Indonesia

930 **Ardiyah Nurul Fitri Marzaman** - Department of Pharmaceutics, Faculty of Pharmacy,  
931 Hasanuddin University, Makassar 90245, Indonesia

932 **Tri Puspita Roska** - Department of Pharmaceutics, Faculty of Pharmacy, Hasanuddin  
933 University, Makassar 90245, Indonesia

934 **Rangga Meidianto Asri** - Department of Pharmaceutics, Faculty of Pharmacy, Hasanuddin  
935 University, Makassar 90245, Indonesia

936 **Achmad Himawan** - Department of Pharmaceutics, Faculty of Pharmacy, Hasanuddin  
937 University, Makassar 90245, Indonesia

938 **Ryan F. Donnelly** - School of Pharmacy, Queen's University Belfast, Medical Biology Centre,  
939 97 Lisburn Road, Belfast. BT9 7BL, UK

940

941

942 Author Contributions

943 The manuscript was written through contributions of all authors. All authors have given

944

945 Notes

946 Ryan Donnelly an inventor of patents that have been licenced to companies developing

947 microneedle-based products and is a paid advisor to companies developing microneedle-based

948 products. The resulting potential conflict of interest has been disclosed and is managed by

949 Queen's University Belfast. The companies had no role in the design of the present studies, in

950 the collection, analyses or interpretation of the data, in the writing of the manuscript or in the

951 decision to publish the work.

952

953 ACKNOWLEDGEMENT

954 Mukarram Mudjahid is thankful for the scholarship provided by German Academic Exchange

955 Service (Deutscher Akademischer Austausch Dienst/DAAD). This Study also was supported

956 by Penelitian Tesis Magister, Ministry of Education, Culture, Research, and Technology of

957 Republic of Indonesia (090/E5/PG.02.00/PT/2022).

958 .

959

960

961

962

963

964

965

966

967

968

969

970 **REFERENCES**

- 971 (1) Clinton, A.; Carter, T. Chronic Wound Biofilms: Pathogenesis and Potential  
972 Therapies. *Lab Med.* **2015**, *46* (4), 277–284.  
973 <https://doi.org/10.1309/LMBNSWKUI4JPN7SO>.
- 974 (2) Rondas, A. A. L. M.; Schols, J. M. G. A.; Stobberingh, E. E.; Halfens, R. J. G.  
975 Prevalence of Chronic Wounds and Structural Quality Indicators of Chronic Wound  
976 Care in Dutch Nursing Homes. *Int. Wound J.* **2015**, *12* (6), 630–635.  
977 <https://doi.org/10.1111/iwj.12172>.
- 978 (3) El-Mohri, H.; Wu, Y.; Mohanty, S.; Ghosh, G. Impact of Matrix Stiffness on  
979 Fibroblast Function. *Mater. Sci. Eng. C* **2017**, *74*, 146–151.  
980 <https://doi.org/10.1016/j.msec.2017.02.001>.
- 981 (4) Raff, A. B.; Kroshinsky, D. Cellulitis A Review. *Jama* **2016**, *316* (3), 325–337.  
982 <https://doi.org/10.1001/jama.2016.8825>.
- 983 (5) Rrapi, R.; Chand, S.; Kroshinsky, D. Cellulitis: A Review of Pathogenesis, Diagnosis,  
984 and Management. *Med. Clin. North Am.* **2021**, *105* (4), 723–735.  
985 <https://doi.org/10.1016/j.mcna.2021.04.009>.
- 986 (6) Andersen, C. A.; McLeod, K.; Steffan, R. Diagnosis and Treatment of the Invasive  
987 Extension of Bacteria (Cellulitis) from Chronic Wounds Utilising Point-of-Care  
988 Fluorescence Imaging. *Int. Wound J.* **2021**, No. September, 1–13.  
989 <https://doi.org/10.1111/iwj.13696>.
- 990 (7) Bou Haidar, N.; Marais, S.; Dé, E.; Schaumann, A.; Barreau, M.; Feuilloy, M. G. J.;  
991 Duncan, A. C. Chronic Wound Healing: A Specific Antibiofilm Protein-Asymmetric  
992 Release System. *Mater. Sci. Eng. C* **2020**, *106* (April 2019).  
993 <https://doi.org/10.1016/j.msec.2019.110130>.
- 994 (8) Mihai, M. M.; Preda, M.; Lungu, I.; Gestal, M. C.; Popa, M. I.; Holban, A. M.

- 995 Nanocoatings for Chronic Wound Repair—Modulation of Microbial Colonization and  
996 Biofilm Formation. *Int. J. Mol. Sci.* **2018**, *19* (4).  
997 <https://doi.org/10.3390/ijms19041179>.
- 998 (9) Gemeinder, J. L. P.; Barros, N. R. de; Pegorin, G. S.; Singulani, J. de L.; Borges, F. A.;  
999 Arco, M. C. G. Del; Giannini, M. J. S. M.; Almeida, A. M. F.; Salvador, S. L. de S.;  
1000 Herculano, R. D. Gentamicin Encapsulated within a Biopolymer for the Treatment of  
1001 Staphylococcus Aureus and Escherichia Coli Infected Skin Ulcers. *J. Biomater. Sci.*  
1002 *Polym. Ed.* **2021**, *32* (1), 93–111. <https://doi.org/10.1080/09205063.2020.1817667>.
- 1003 (10) Sartini, S.; Permana, A. D.; Mitra, S.; Tareq, A. M.; Salim, E.; Ahmad, I.; Harapan, H.;  
1004 Emran, T. Bin; Nainu, F. Current State and Promising Opportunities on  
1005 Pharmaceutical Approaches in the Treatment of Polymicrobial Diseases. *Pathogens*  
1006 **2021**, *10* (2), 1–31. <https://doi.org/10.3390/pathogens10020245>.
- 1007 (11) Kalita, S.; Devi, B.; Kandimalla, R.; Sharma, K. K.; Sharma, A.; Kalita, K.; Kataki, A.  
1008 C.; Kotoky, J. Chloramphenicol Encapsulated in Poly- $\epsilon$ -Caprolactone-Pluronic  
1009 Composite: Nanoparticles for Treatment of MRSA-Infected Burn Wounds. *Int. J.*  
1010 *Nanomedicine* **2015**, *10*, 2971–2984. <https://doi.org/10.2147/IJN.S75023>.
- 1011 (12) Abdollahi, M.; Mostafalou, S. Chloramphenicol. *Encycl. Toxicol. Third Ed.* **2014**, *1*,  
1012 837–840. <https://doi.org/10.1016/B978-0-12-386454-3.00709-0>.
- 1013 (13) Shukla, P.; Bansode, F. W.; Singh, R. K. Chloramphenicol Toxicity : A Review. *J.*  
1014 *Med. Med. Sci.* **2011**, *2* (13), 1313–1316.
- 1015 (14) Allen, T. M.; Cullis, P. R. Drug Delivery Systems: Entering the Mainstream. *Science*  
1016 (80-. ). **2004**, *303* (5665), 1818–1822. <https://doi.org/10.1126/science.1095833>.
- 1017 (15) Chatterjee, S.; Hui, P. C. leung. Review of Stimuli-Responsive Polymers in Drug  
1018 Delivery and Textile Application. *Molecules* **2019**, *24* (14).  
1019 <https://doi.org/10.3390/molecules24142547>.

- 1020 (16) Ayaz, P.; Xu, B.; Zhang, X.; Wang, J.; Yu, D.; Wu, J. A PH and Hyaluronidase Dual-  
1021 Responsive Multilayer-Based Drug Delivery System for Resisting Bacterial Infection.  
1022 *Appl. Surf. Sci.* **2020**, 527 (February), 146806.  
1023 <https://doi.org/10.1016/j.apsusc.2020.146806>.
- 1024 (17) Xiong, M. H.; Bao, Y.; Yang, X. Z.; Wang, Y. C.; Sun, B.; Wang, J. Lipase-Sensitive  
1025 Polymeric Triple-Layered Nanogel for “on-Demand” Drug Delivery. *J. Am. Chem.*  
1026 *Soc.* **2012**, 134 (9), 4355–4362. <https://doi.org/10.1021/ja211279u>.
- 1027 (18) Ferreira, I. S.; Bettencourt, A. F.; Gonçalves, L. M. D.; Kasper, S.; Bétrisey, B.;  
1028 Kikhney, J.; Moter, A.; Trampuz, A.; Almeida, A. J. Activity of Daptomycin- and  
1029 Vancomycin-Loaded Poly-Epsilon-Caprolactone Microparticles against Mature  
1030 Staphylococcal Biofilms. *Int. J. Nanomedicine* **2015**, 10, 4351–4366.  
1031 <https://doi.org/10.2147/IJN.S84108>.
- 1032 (19) Permana, A. D.; Nainu, F.; Moffatt, K.; Larrañeta, E.; Donnelly, R. F. Recent  
1033 Advances in Combination of Microneedles and Nanomedicines for Lymphatic  
1034 Targeted Drug Delivery. *Wiley Interdiscip. Rev. Nanomedicine Nanobiotechnology*  
1035 **2021**, 13 (3), 1–22. <https://doi.org/10.1002/wnan.1690>.
- 1036 (20) Permana, A. D.; Anjani, Q. K.; Sartini; Utomo, E.; Volpe-Zanutto, F.; Paredes, A. J.;  
1037 Evary, Y. M.; Mardikasari, S. A.; Pratama, M. R.; Tuany, I. N.; Donnelly, R. F.  
1038 Selective Delivery of Silver Nanoparticles for Improved Treatment of Biofilm Skin  
1039 Infection Using Bacteria-Responsive Microparticles Loaded into Dissolving  
1040 Microneedles. *Mater. Sci. Eng. C* **2021**, 120 (November 2020), 111786.  
1041 <https://doi.org/10.1016/j.msec.2020.111786>.
- 1042 (21) Lengyel, M.; Kállai-Szabó, N.; Antal, V.; Laki, A. J.; Antal, I. Microparticles,  
1043 Microspheres, and Microcapsules for Advanced Drug Delivery. *Sci. Pharm.* **2019**, 87  
1044 (3). <https://doi.org/10.3390/scipharm87030020>.

- 1045 (22) Kalita, S.; Devi, B.; Kandimalla, R.; Sharma, K. K.; Sharma, A.; Kalita, K.; Kataki, A.  
1046 C.; Kotoky, J. Chloramphenicol Encapsulated in Poly- $\epsilon$ - Caprolactone–Pluronic  
1047 Composite Nanoparticles for Treatment of Mrsa-Infected Burn Wounds.Pdf. 2015.
- 1048 (23) Permana, A. D.; McCrudden, M. T. C.; Donnelly, R. F. Enhanced Intradermal  
1049 Delivery of Nanosuspensions of Antifilariasis Drugs Using Dissolving Microneedles:  
1050 A Proof of Concept Study. *Pharmaceutics* **2019**, *11* (7), 1–22.  
1051 <https://doi.org/10.3390/pharmaceutics11070346>.
- 1052 (24) Ita, K. Dissolving Microneedles for Transdermal Drug Delivery: Advances and  
1053 Challenges. *Biomed. Pharmacother.* **2017**, *93*, 1116–1127.  
1054 <https://doi.org/10.1016/j.biopha.2017.07.019>.
- 1055 (25) Permana, A. D.; Tekko, I. A.; McCrudden, M. T. C.; Anjani, Q. K.; Ramadan, D.;  
1056 McCarthy, H. O.; Donnelly, R. F. Solid Lipid Nanoparticle-Based Dissolving  
1057 Microneedles: A Promising Intradermal Lymph Targeting Drug Delivery System with  
1058 Potential for Enhanced Treatment of Lymphatic Filariasis. *J. Control. Release* **2019**,  
1059 *316* (September), 34–52. <https://doi.org/10.1016/j.jconrel.2019.10.004>.
- 1060 (26) Badran, M. M.; Alomrani, A. H.; Harisa, G. I.; Ashour, A. E.; Kumar, A.; Yassin, A.  
1061 E. Novel Docetaxel Chitosan-Coated PLGA/PCL Nanoparticles with Magnified  
1062 Cytotoxicity and Bioavailability. *Biomed. Pharmacother.* **2018**, *106* (July), 1461–  
1063 1468. <https://doi.org/10.1016/j.biopha.2018.07.102>.
- 1064 (27) Yang, Z. G.; Sun, H. X.; Fang, W. H. Haemolytic Activities and Adjuvant Effect of  
1065 Astragalus Membranaceus Saponins (AMS) on the Immune Responses to Ovalbumin  
1066 in Mice. *Vaccine* **2005**, *23* (44), 5196–5203.  
1067 <https://doi.org/10.1016/j.vaccine.2005.06.016>.
- 1068 (28) Radaelli, M.; da Silva, B. P.; Weidlich, L.; Hoehne, L.; Flach, A.; da Costa, L. A. M.  
1069 A.; Ethur, E. M. Antimicrobial Activities of Six Essential Oils Commonly Used as

- 1070 Condiments in Brazil against *Clostridium Perfringens*. *Brazilian J. Microbiol.* **2016**,  
1071 47 (2), 424–430. <https://doi.org/10.1016/j.bjm.2015.10.001>.
- 1072 (29) Chen, H.; Li, L.; Liu, Y.; Wu, M.; Xu, S.; Zhang, G.; Qi, C.; Du, Y.; Wang, M.; Li, J.;  
1073 Huang, X. In Vitro Activity and Post-Antibiotic Effects of Linezolid in Combination  
1074 with Fosfomycin against Clinical Isolates of *Staphylococcus Aureus*. *Infect. Drug*  
1075 *Resist.* **2018**, 11, 2107–2115. <https://doi.org/10.2147/IDR.S175978>.
- 1076 (30) Ramond, E.; Jamet, A.; Ding, X.; Euphrasie, D.; Bouvier, C.; Lallemand, L.; He, X.;  
1077 Arbibe, L.; Coureuil, M.; Charbit, A. Reactive Oxygen Species-Dependent Innate  
1078 Immune Mechanisms Control Methicillin-Resistant *Staphylococcus Aureus* Virulence  
1079 in the *Drosophila* Larval Model. *MBio* **2021**, 12 (3).  
1080 <https://doi.org/10.1128/mBio.00276-21>.
- 1081 (31) Zhang, Y.; Huo, M.; Zhou, J.; Xie, S. PKSolver: An Add-in Program for  
1082 Pharmacokinetic and Pharmacodynamic Data Analysis in Microsoft Excel. *Comput.*  
1083 *Methods Programs Biomed.* **2010**, 99 (3), 306–314.  
1084 <https://doi.org/10.1016/j.cmpb.2010.01.007>.
- 1085 (32) Putri, H. E.; Utami, R. N.; Aliyah; Wahyudin, E.; Oktaviani, W. W.; Mudjahid, M.;  
1086 Permana, A. D. Dissolving Microneedle Formulation of Ceftriaxone: Effect of  
1087 Polymer Concentrations on Characterisation and Ex Vivo Permeation Study. *J. Pharm.*  
1088 *Innov.* **2021**, No. 0123456789. <https://doi.org/10.1007/s12247-021-09593-y>.
- 1089 (33) Permana, A. D.; Paredes, A. J.; Volpe-Zanutto, F.; Anjani, Q. K.; Utomo, E.;  
1090 Donnelly, R. F. Dissolving Microneedle-Mediated Dermal Delivery of Itraconazole  
1091 Nanocrystals for Improved Treatment of Cutaneous Candidiasis. *Eur. J. Pharm.*  
1092 *Biopharm.* **2020**, 154 (June), 50–61. <https://doi.org/10.1016/j.ejpb.2020.06.025>.
- 1093 (34) González-Vázquez, P.; Larrañeta, E.; McCrudden, M. T. C.; Jarrahian, C.; Rein-  
1094 Weston, A.; Quintanar-Solares, M.; Zehrun, D.; McCarthy, H.; Courtenay, A. J.;

- 1095 Donnelly, R. F. Transdermal Delivery of Gentamicin Using Dissolving Microneedle  
1096 Arrays for Potential Treatment of Neonatal Sepsis. *J. Control. Release* **2017**, *265*, 30–  
1097 40. <https://doi.org/10.1016/j.jconrel.2017.07.032>.
- 1098 (35) Alhusein, N.; Blagbrough, I. S.; Beeton, M. L.; Bolhuis, A.; De Bank, P. A.  
1099 Electrospun Zein/PCL Fibrous Matrices Release Tetracycline in a Controlled Manner,  
1100 Killing *Staphylococcus Aureus* Both in Biofilms and Ex Vivo on Pig Skin, and Are  
1101 Compatible with Human Skin Cells. *Pharm. Res.* **2016**, *33* (1), 237–246.  
1102 <https://doi.org/10.1007/s11095-015-1782-3>.
- 1103 (36) Roche, E. D.; Woodmansey, E. J.; Yang, Q.; Gibson, D. J.; Zhang, H.; Schultz, G. S.  
1104 Cadexomer Iodine Effectively Reduces Bacterial Biofilm in Porcine Wounds Ex Vivo  
1105 and in Vivo. *Int. Wound J.* **2019**, *16* (3), 674–683. <https://doi.org/10.1111/iwj.13080>.
- 1106 (37) Mir, M.; Ishtiaq, S.; Rabia, S.; Khatoun, M.; Zeb, A.; Khan, G. M.; ur Rehman, A.; ud  
1107 Din, F. Nanotechnology: From In Vivo Imaging System to Controlled Drug Delivery.  
1108 *Nanoscale Res. Lett.* **2017**, *12*. <https://doi.org/10.1186/s11671-017-2249-8>.
- 1109 (38) Ahmadi, M.; Vahabzadeh, F.; Bonakdarpour, B.; Mofarrah, E.; Mehranian, M.  
1110 Application of the Central Composite Design and Response Surface Methodology to  
1111 the Advanced Treatment of Olive Oil Processing Wastewater Using Fenton’s  
1112 Peroxidation. *J. Hazard. Mater.* **2005**, *123* (1–3), 187–195.  
1113 <https://doi.org/10.1016/j.jhazmat.2005.03.042>.
- 1114 (39) Budhian, A.; Siegel, S. J.; Winey, K. I. Haloperidol-Loaded PLGA Nanoparticles:  
1115 Systematic Study of Particle Size and Drug Content. *Int. J. Pharm.* **2007**, *336* (2),  
1116 367–375. <https://doi.org/10.1016/j.ijpharm.2006.11.061>.
- 1117 (40) Dubey, N.; Varshney, R.; Shukla, J.; Ganeshpurkar, A.; Hazari, P. P.; Bandopadhaya,  
1118 G. P.; Mishra, A. K.; Trivedi, P. Synthesis and Evaluation of Biodegradable PCL/PEG  
1119 Nanoparticles for Neuroendocrine Tumor Targeted Delivery of Somatostatin Analog.

- 1120 *Drug Deliv.* **2012**, *19* (3), 132–142. <https://doi.org/10.3109/10717544.2012.657718>.
- 1121 (41) Shalaby, K. S.; Soliman, M. E.; Casettari, L.; Bonacucina, G.; Cespi, M.; Palmieri, G.  
1122 F.; Sammour, O. A.; El Shamy, A. A. Determination of Factors Controlling the  
1123 Particle Size and Entrapment Efficiency of Noscapine in PEG/PLA Nanoparticles  
1124 Using Artificial Neural Networks. *Int. J. Nanomedicine* **2014**, *9* (1), 4953–4964.  
1125 <https://doi.org/10.2147/IJN.S68737>.
- 1126 (42) Mahmoudi, M.; Saeidian, H.; Mirjafary, Z.; Mokhtari, J. Preparation and  
1127 Characterization of Memantine Loaded Polycaprolactone Nanocapsules for  
1128 Alzheimer's Disease. *J. Porous Mater.* **2021**, *28* (1), 205–212.  
1129 <https://doi.org/10.1007/s10934-020-00981-2>.
- 1130 (43) Pajerski, W.; Ochonska, D.; Brzychczy-Wloch, M.; Indyka, P.; Jarosz, M.; Golda-  
1131 Cepa, M.; Sojka, Z.; Kotarba, A. Attachment Efficiency of Gold Nanoparticles by  
1132 Gram-Positive and Gram-Negative Bacterial Strains Governed by Surface Charges. *J.*  
1133 *Nanoparticle Res.* **2019**, *21* (8). <https://doi.org/10.1007/s11051-019-4617-z>.
- 1134 (44) Halder, S.; Yadav, K. K.; Sarkar, R.; Mukherjee, S.; Saha, P.; Haldar, S.; Karmakar,  
1135 S.; Sen, T. Alteration of Zeta Potential and Membrane Permeability in Bacteria: A  
1136 Study with Cationic Agents. *Springerplus* **2015**, *4* (1), 1–14.  
1137 <https://doi.org/10.1186/s40064-015-1476-7>.
- 1138 (45) Zhou, H. Y.; Zhang, Y. P.; Zhang, W. F.; Chen, X. G. Biocompatibility and  
1139 Characteristics of Injectable Chitosan-Based Thermosensitive Hydrogel for Drug  
1140 Delivery. *Carbohydr. Polym.* **2011**, *83* (4), 1643–1651.  
1141 <https://doi.org/10.1016/j.carbpol.2010.10.022>.
- 1142 (46) Chen, H.; Jin, Y.; Wang, J.; Wang, Y.; Jiang, W.; Dai, H.; Pang, S.; Lei, L.; Ji, J.;  
1143 Wang, B. Design of Smart Targeted and Responsive Drug Delivery Systems with  
1144 Enhanced Antibacterial Properties. *Nanoscale* **2018**, *10* (45), 20946–20962.

- 1145 <https://doi.org/10.1039/c8nr07146b>.
- 1146 (47) Wu, C.; Jim, T. F.; Gan, Z.; Zhao, Y.; Wang, S. A Heterogeneous Catalytic Kinetics  
1147 for Enzymatic Biodegradation of Poly (  $\epsilon$ -Caprolactone ) Nanoparticles in Aqueous  
1148 Solution. **2000**, *41*, 3593–3597.
- 1149 (48) Laracuenta, M. L.; Yu, M. H.; McHugh, K. J. Zero-Order Drug Delivery: State of the  
1150 Art and Future Prospects. *J. Control. Release* **2020**, *327*, 834–856.  
1151 <https://doi.org/10.1016/j.jconrel.2020.09.020>.
- 1152 (49) Clinical and Laboratory Standards Institute (CLSI). Performance Standards for  
1153 Antimicrobial Susceptibility Testing; Twenty-Second Informational Supplement  
1154 (M100-S22). Wayne, PA: CLSI; 2012.
- 1155 (50) Tato, M.; López, Y.; Morosini, M. I.; Moreno-Bofarull, A.; Garcia-Alonso, F.;  
1156 Gargallo-Viola, D.; Vila, J.; Cantón, R. Characterization of Variables That May  
1157 Influence Ozenoxacin in Susceptibility Testing, Including MIC and MBC Values.  
1158 *Diagn. Microbiol. Infect. Dis.* **2014**, *78* (3), 263–267.  
1159 <https://doi.org/10.1016/j.diagmicrobio.2013.11.010>.
- 1160 (51) Buchon, N.; Silverman, N.; Cherry, S. Immunity in *Drosophila Melanogaster*-from  
1161 Microbial Recognition to Whole-Organism Physiology. *Nat. Rev. Immunol.* **2014**, *14*  
1162 (12), 796–810. <https://doi.org/10.1038/nri3763>.
- 1163 (52) Nainu, F.; Natsir Djide, M.; Subehan; Sartini; Roska, T. P.; Salim, E.; Kuraishi, T.  
1164 Protective Signatures of Roselle (*Hibiscus Sabdariffa* L.) Calyx Fractions against  
1165 *Staphylococcus Aureus* in *Drosophila* Infection Model. *HAYATI J. Biosci.* **2020**, *27*  
1166 (4), 306–313. <https://doi.org/10.4308/hjb.27.4.306>.
- 1167 (53) Chamy, L. El; Leclerc, V.; Caldelari, I.; Reichhart, J. M. Sensing of “danger Signals”  
1168 and Pathogen-Associated Molecular Patterns Defines Binary Signaling Pathways  
1169 “Upstream” of Toll. *Nat. Immunol.* **2008**, *9* (10), 1165–1170.

1170 <https://doi.org/10.1038/ni.1643>.

1171 (54) Buchon, N.; Poidevin, M.; Kwon, H. M.; Guillou, A. L.; Sottas, V.; Lee, B. L.;  
1172 Lemaitrea, B. A Single Modular Serine Protease Integrates Signals from Pattern-  
1173 Recognition Receptors Upstream of the Drosophila Toll Pathway. *Proc. Natl. Acad.*  
1174 *Sci. U. S. A.* **2009**, *106* (30), 12442–12447. <https://doi.org/10.1073/pnas.0901924106>.

1175 (55) Larrañeta, E.; Moore, J.; Vicente-Pérez, E. M.; González-Vázquez, P.; Lutton, R.;  
1176 Woolfson, A. D.; Donnelly, R. F. A Proposed Model Membrane and Test Method for  
1177 Microneedle Insertion Studies. *Int. J. Pharm.* **2014**, *472* (1–2), 65–73.  
1178 <https://doi.org/10.1016/j.ijpharm.2014.05.042>.

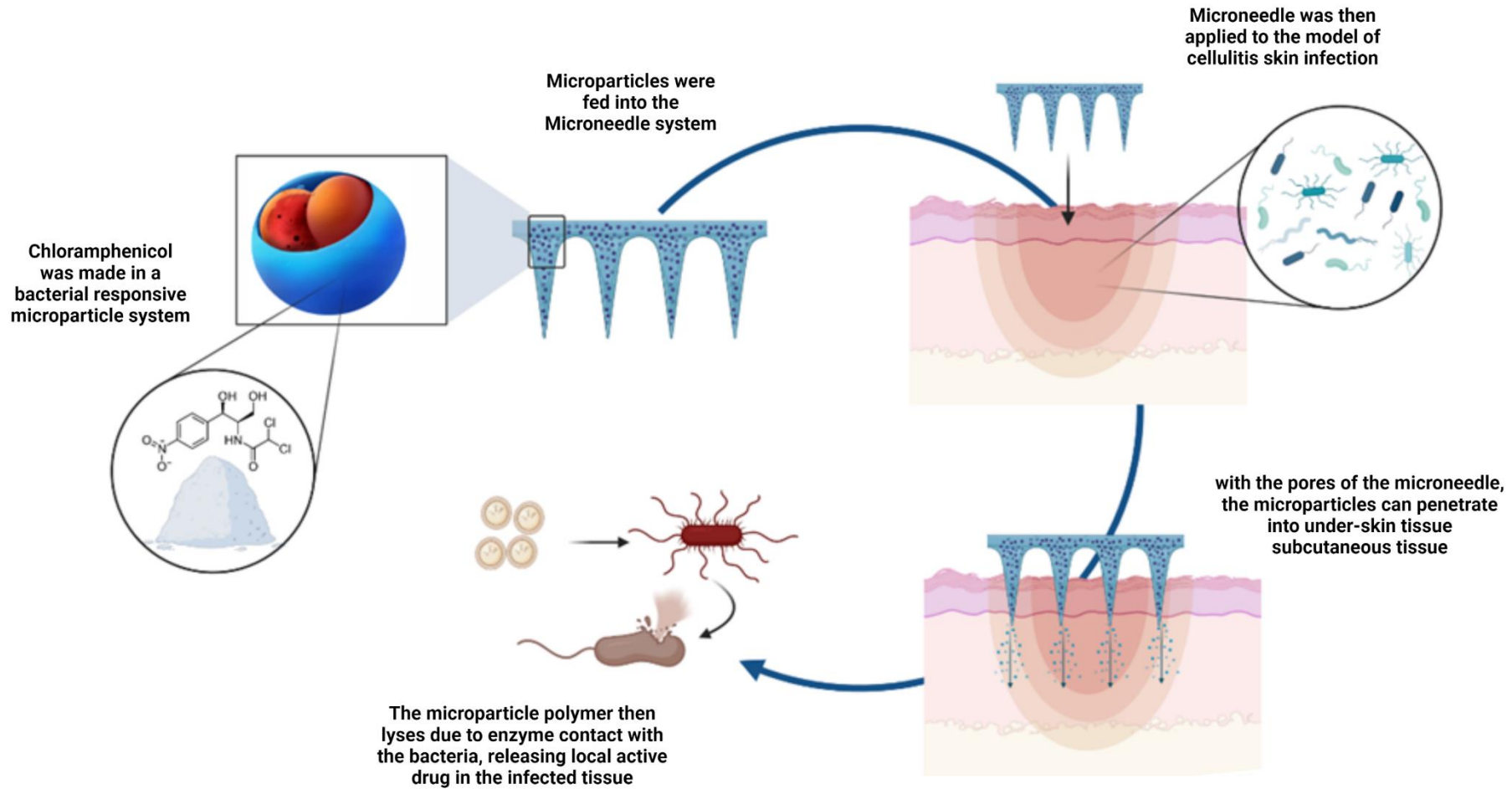
1179 (56) Pamornpathomkul, B.; Ngawhirunpat, T.; Tekko, I. A.; Vora, L.; McCarthy, H. O.;  
1180 Donnelly, R. F. Dissolving Polymeric Microneedle Arrays for Enhanced Site-Specific  
1181 Acyclovir Delivery. *Eur. J. Pharm. Sci.* **2018**, *121* (April), 200–209.  
1182 <https://doi.org/10.1016/j.ejps.2018.05.009>.

1183 (57) Permana, A. D.; Mir, M.; Utomo, E.; Donnelly, R. F. Bacterially Sensitive  
1184 Nanoparticle-Based Dissolving Microneedles of Doxycycline for Enhanced Treatment  
1185 of Bacterial Biofilm Skin Infection: A Proof of Concept Study. *International Journal*  
1186 *of Pharmaceutics: X.* 2020. <https://doi.org/10.1016/j.ijpx.2020.100047>.

1187 (58) Mir, M.; Ahmed, N.; Permana, A. D.; Rodgers, A. M.; Donnelly, R. F.; Rehman, A. U.  
1188 Enhancement in Site-Specific Delivery of Carvacrol against Methicillin Resistant  
1189 Staphylococcus Aureus Induced Skin Infections Using Enzyme Responsive  
1190 Nanoparticles: A Proof of Concept Study. *Pharmaceutics.* 2019.  
1191 <https://doi.org/10.3390/pharmaceutics11110606>.

1192  
1193

## Table of Contents Graphic



**BUKTI**  
**ACCEPTED**



Andi Dian Permana &lt;andi.dian.permana@farmasi.unhas.ac.id&gt;

---

**Decision on Manuscript ID am-2022-16857x.R1**2 messages

---

**ACS Applied Materials & Interfaces** <onbehalf@manuscriptcentral.com>

Thu, Dec 1, 2022 at 2:44 AM

Reply-To: ivanisevic-office@ami.acs.org

To: andi.dian.permana@farmasi.unhas.ac.id

30-Nov-2022

Journal: ACS Applied Materials &amp; Interfaces

Manuscript ID: am-2022-16857x.R1

Title: "Enhancement in Site-Specific Delivery of Chloramphenicol Using Bacterially Sensitive Microparticle Loaded Into Dissolving Microneedle : Potential For Enhanced Effectiveness Treatment of Cellulitis"

Authors: Mudjahid, Mukarram ; Nainu, Firzan; Utami, Rifka; Sam, Anwar; Marzaman, Ardiyah; Roska, Tri; Asri, Rangga; Himawan, Achmad; Donnelly, Ryan F.; Permana, Andi Dian

Manuscript Status: Accept

Dear Dr. Permana:

We are pleased to inform you that your manuscript has been accepted for publication in ACS Applied Materials & Interfaces.

You will soon receive an email invitation from the ACS Journal Publishing Staff that contains a link to the online Journal Publishing Agreement. Please sign and submit the journal publishing agreement within 48 hours.

Your manuscript has been forwarded to the ACS Publications office. You will be contacted in the near future by the ACS Journal Publishing Staff regarding the proofs for your manuscript.

After you approve your proofs, your manuscript will be published on the Web in approximately 48 hours. In view of this fast publication time, it is important to review your proofs carefully. Once a manuscript appears on the Web it is considered published. Any change to the manuscript once it appears on the Web will need to be submitted to the journal office as additions or corrections.

Once your paper is published, you can track downloads and citations of your work by logging into the ACS Publishing Center (<https://pubs.acs.org/publish/dashboard>) and selecting "Published".

Sincerely,

Prof. Albena Ivanisevic  
Associate Editor  
ACS Applied Materials & Interfaces  
Fax: 12023509587  
email: [ivanisevic-office@ami.acs.org](mailto:ivanisevic-office@ami.acs.org)

-----  
TWITTER: ACS Applied Materials & Interfaces has a Twitter account (@ACS\_AMI). If you would like us to tweet about your article when it appears on ASAP, please recommend a tweet of less than 200 characters to [ami-social@ami.acs.org](mailto:ami-social@ami.acs.org), with your Manuscript ID number (e.g., am-2020-XXXXXX) as the subject line. Include any relevant Twitter handles you would like to include; you do not need to include any DOI or URL information. If you wish to use a graphic other than the TOC graphic, please send it as an attachment. We may modify the tweet before posting, and we may not be able to include all tweets submitted. We appreciate your willingness to provide the tweet within one week of receipt of this email.

-----  
PLEASE NOTE: This email message, including any attachments, contains confidential information related to peer review and is intended solely for the personal use of the recipient(s) named above. No part of this communication or any related attachments may be shared with or disclosed to any third party or organization without the explicit prior written consent of the journal Editor and ACS. If the reader of this message is not the intended recipient or is not responsible for delivering it to the intended recipient, you have received this communication in error. Please notify the sender immediately by e-mail, and delete the original message.

As an author or reviewer for ACS Publications, we may send you communications about related journals, topics or products and services from the American Chemical Society. Please email us at [pubs-comms-unsub@acs.org](mailto:pubs-comms-unsub@acs.org) if you do not want to receive these. Note, you will still receive updates about your manuscripts, reviews, or future invitations to review.

Thank you.

---

**Andi Dian Permana** <[andi.dian.permana@farmasi.unhas.ac.id](mailto:andi.dian.permana@farmasi.unhas.ac.id)>  
To: Ryan Donnelly <[r.donnelly@qub.ac.uk](mailto:r.donnelly@qub.ac.uk)>

Thu, Dec 1, 2022 at 4:37 AM

Hi Ryan,

Please see email below

Thank you for your support.

Best wishes,  
Dian

[Quoted text hidden]